






The SiaA/B/C/D signaling network regulates biofilm formation in *Pseudomonas aeruginosa*

Gukui Chen^{1,†} , Jianhua Gan^{2,†} , Chun Yang², Yili Zuo¹, Juan Peng¹, Meng Li¹ , Weiping Huo¹, Yingpeng Xie³, Yani Zhang¹, Tietao Wang¹ , Xin Deng³ & Haihua Liang^{1,*} 

Abstract

Bacterial cyclic-di-GMP (c-di-GMP) production is associated with biofilm development and the switch from acute to chronic infections. In *Pseudomonas aeruginosa*, the diguanylate cyclase (DGC) SiaD and phosphatase SiaA, which are co-transcribed as part of a *siaABCD* operon, are essential for cellular aggregation. However, the detailed functions of this operon and the relationships among its constituent genes are unknown. Here, we demonstrate that the *siaABCD* operon encodes for a signaling network that regulates SiaD enzymatic activity to control biofilm and aggregates formation. Through protein–protein interaction, SiaC promotes SiaD diguanylate cyclase activity. Biochemical and structural data revealed that SiaB is an unusual protein kinase that phosphorylates SiaC, whereas SiaA phosphatase can dephosphorylate SiaC. The phosphorylation state of SiaC is critical for its interaction with SiaD, which will switch on or off the DGC activity of SiaD and regulate c-di-GMP levels and subsequent virulence phenotypes. Collectively, our data provide insights into the molecular mechanisms underlying the modulation of DGC activity associated with chronic infections, which may facilitate the development of antimicrobial drugs.

Keywords biofilm formation; crystal structure; phosphorylation; protein–protein interaction; *Pseudomonas aeruginosa*

Subject Categories Microbiology, Virology & Host Pathogen Interaction; Post-translational Modifications & Proteolysis; Signal Transduction

DOI 10.15252/embj.2019103412 | Received 8 September 2019 | Revised 21 January 2020 | Accepted 3 February 2020 | Published online 24 February 2020

The EMBO Journal (2020) 39: e103412

Introduction

The intracellular messenger cyclic dimeric (3′–5′) GMP (cyclic di-GMP or c-di-GMP) is a small molecule that mediates various aspects of the physiology of diverse environmental and pathogenic bacteria

(Romling *et al.*, 2013; Jenal *et al.*, 2017). It was first described in 1986 as an allosteric factor that activated cellulose synthase in *Acetobacter xylinum* (Ross *et al.*, 1987). To date, c-di-GMP has been shown to regulate the cell cycle, biofilm formation and dispersion, motility, virulence, and other processes (Romling *et al.*, 2013; Jenal *et al.*, 2017). C-di-GMP promotes biofilm growth by stimulating the production of exopolysaccharide (EPS) and adhesins (Simm *et al.*, 2004; Jenal *et al.*, 2017). C-di-GMP is synthesized by diguanylate cyclases (DGCs) harboring a GGDEF domain (Simm *et al.*, 2004; Schmidt *et al.*, 2005). Degradation of c-di-GMP is catalyzed by phosphodiesterases (PDE) with an EAL or HD-GYP domain, which results in the production of 5-phosphoguanylyl-(3′,5′)-guanosine (pGpG) or GMP (Simm *et al.*, 2004). pGpG is further hydrolyzed by oligoribonucleases into two GMP molecules (Cohen *et al.*, 2015; Orr *et al.*, 2015).

The c-di-GMP regulatory system in *Pseudomonas aeruginosa* is highly sophisticated. The genome of *P. aeruginosa* PAO1 contains 17 genes with a predicted DGC domain, 5 with a PDE domain, and 16 with both domains (Kulasakara *et al.*, 2006). SiaD contains a DGC domain that is essential for cell aggregation, a bacterial stress response that promotes the survival of *P. aeruginosa* in response to the toxic detergent sodium dodecylsulfate (SDS) (Klebensberger *et al.*, 2009). This process requires the putative inner membrane-located Ser/Thr phosphatase SiaA, which contains two transmembrane helices, a HAMP domain and a sigma factor PP2C-like phosphatase domain. SiaA and SiaD also regulate the Psl polysaccharide, the CdrAB two-partner secretion system, and the CupA fimbriae (Klebensberger *et al.*, 2009). Recently, Chew *et al.* (2018) have reported that SiaD is required for the competitiveness of *P. aeruginosa* during dual-species biofilm development with *Staphylococcus aureus*. Additionally, SiaA and SiaD functionally interact with the RsmA post-transcriptional regulatory system, which is known to control motility, biofilm formation, and cell aggregation (Brencic & Lory, 2009; Colley *et al.*, 2016). SiaA and SiaD regulate the RsmA antagonist *rsmZ* during growth with SDS, whereas RsmA controls *siaD* transcription (Colley *et al.*, 2016).

In all kingdoms of life, reversible protein phosphorylation controls the activity of enzymes, or the association of proteins with

¹ Key Laboratory of Resources Biology and Biotechnology in Western China, Ministry of Education, College of Life Sciences, Northwest University, Xi'an, Shaanxi, China

² State Key Laboratory of Genetic Engineering, Shanghai Public Health Clinical Center, Collaborative Innovation Center of Genetics and Development, School of Life Sciences, Fudan University, Shanghai, China

³ Department of Biomedical Sciences, City University of Hong Kong, Hong Kong, China

*Corresponding author. Tel: +86 029 88303662. E-mail: lianghh@nwu.edu.cn

[†]These authors contributed equally to this work

other proteins (Hunter, 1995). Phosphoryl groups, typically originating from ATP, are attached to amino acid side chains on protein by protein kinases, and are removed by protein phosphatases in response to specific cellular or environmental cues; therefore, reversible phosphorylation controls diverse biological processes (Taylor & Kornev, 2011). Phosphorylation and DGC activity crosstalk have been reported to control c-di-GMP production. The DGC activity of WspR is induced via phosphorylation by the Wsp chemosensory system in response to growth of *P. aeruginosa* on surface (Hickman et al., 2005). Active WspR then produces c-di-GMP to stimulate biofilm formation. In *Bdellovibrio bacteriovorus*, the DGC activity of DgcB is dependent on the sensory fork head-associated (FHA) domain bound with the ligand from the N-terminal region of DgcB itself (Meek et al., 2019). The MtG DGC activity in *Moorella thermoacetica* is modulated by the stressosome complex and the switch kinase MtT (Quin et al., 2012). Here, we report that SiaC and SiaB function together with SiaD and SiaA to regulate biofilm formation by modulating the intracellular c-di-GMP levels. We demonstrate that SiaC acts as a binding partner to regulate the DGC activity of SiaD. Structural and biochemical data show that SiaB is a kinase that phosphorylates SiaC and the phosphatase SiaA dephosphorylates it at the same site. The reversible phosphorylation of SiaC plays an essential role in the activity of SiaD and subsequent biofilm and aggregate formation. Taken together, this study uncovers SiaC as a key “switch” of the signaling pathway and elucidates a novel phospho-signaling regulatory mechanism underlying the DGC activity by SiaC.

Results

SiaC and SiaB inversely regulates biofilm and aggregate formation through SiaD

SiaA and SiaD are essential for SDS-induced formation of macroscopic aggregates in *P. aeruginosa* (Klebensberger et al., 2009). Furthermore, *siaA* (PA0172) and *siaD* (PA0169) are co-transcribed with *siaB* (PA0171) and *siaC* (PA0170), which encode proteins with

unknown functions (Klebensberger et al., 2009). This information led us to test whether SiaC and SiaB play a role in SDS-induced aggregation. To this end, the deletion mutants of $\Delta siaC$ and $\Delta siaB$ were generated. Similar to the $\Delta siaA$ and $\Delta siaD$ mutants, phenotypic characterization of the $\Delta siaC$ mutant during growth in M9 salt with SDS as the sole carbon source revealed the decreased formation of macroscopic aggregates compared to the PAO1 strain (Appendix Fig S1A; Klebensberger et al., 2009). However, the $\Delta siaB$ mutant exhibited enhanced macroscopic aggregation in M9 salt with SDS, and expression of *siaC* or *siaB* *in trans* in the corresponding mutant restored formation of macroscopic aggregates (Appendix Fig S1A). SDS-induced aggregation is linked to c-di-GMP, a ubiquitous bacterial second messenger that regulates the transition between motile and sessile biofilm lifestyles (Klebensberger et al., 2009). Therefore, we tested whether both SiaC and SiaB regulated the formation of biofilm. As shown in Fig 1A, the ability to form biofilm of $\Delta siaC$ was drastically decreased compared to that of wild-type parent. By contrast, deletion of *siaB* promoted biofilm formation, which was consistent with the SiaB-mediated aggregation. Indeed, expression of *siaC* and *siaB* *in trans* in the corresponding mutant exhibited increased or reduced biofilm formation compared to that of wild-type strain, respectively (Fig 1A). As expected, deletion of *siaA* or *siaD* impaired biofilm formation (Fig 1A). These data demonstrated that SiaA, SiaC, and SiaD positively, and SiaB negatively, regulate macroscopic aggregation and biofilm formation, suggesting the cooperative function of these proteins in regulating these processes.

The c-di-GMP signal has been shown to be involved in *P. aeruginosa* macroscopic aggregation and biofilm formation (Klebensberger et al., 2009; Zhu et al., 2016a). Therefore, we sought to determine whether SiaB and SiaC influence the intracellular level of c-di-GMP. To this end, we measured the concentration of intracellular c-di-GMP via LC-MS/MS, which showed that the $\Delta siaC$ produced less but $\Delta siaB$ had more c-di-GMP than the wild-type strain (Fig 1B). The mRNA levels of *cdrA*, which is responsive to intracellular level of c-di-GMP (Baraquet et al., 2012), were also determined by quantitative reverse transcription-polymerase chain reaction (qRT-PCR) and gain similar trends (Appendix Fig S1B). In addition,

Figure 1. SiaB and SiaC regulate biofilm formation by modulating intracellular c-di-GMP levels through SiaD.

- A Deletion of *siaA*, *siaB*, *siaC*, or *siaD* regulates biofilm formation. The biofilm formation of the indicated strains was displayed with crystal violet staining (up) and quantified with optical density measurement (down).
- B The intracellular levels of c-di-GMP in PAO1, $\Delta siaC$, $\Delta siaB$, and the corresponding complemented strains were detected by LC-MS/MS.
- C SiaB- and SiaC-regulated biofilm formation is dependent on SiaD. Biofilm formation by the indicated strains was displayed with crystal violet staining (up) and quantified with optical density measurement (down).
- D SiaC is required for the function of SiaD. Biofilm formation by the indicated strains was displayed with crystal violet staining (up) and quantified with optical density measurement (down).
- E Bacterial two-hybrid assay reveals an interaction between SiaC and SiaD. The recombinant strains harboring different vectors were separately streaked on nonselective and dual-selective media (3-amino-1, 2, 4- triazole + streptomycin). NA represents the empty vector pBT or pTRG. The strain-expressing LGF2 and Gal11^P were used as positive controls.
- F Pull-down assays confirmed the interaction between SiaC and SiaD. Cell lysates of *Pseudomonas aeruginosa* containing pMM67EH-*siaD*-Flag were incubated with GST or GST-SiaC individually, and protein complexes were captured by glutathione beads.
- G SPR measurements of SiaC (left) or SiaC^P (right) binding at varying concentrations to SiaD. SiaC specifically interacted with SiaD with a K_D of 24.7 nM, whereas SiaC^P failed to interact with SiaB. Shown are measured binding responses (black) and curve fits to a 1:1 interaction (red). Plots are representative of two experiments with similar results. RU, response units; K_D , dissociation constant.
- H Production of c-di-GMP by either SiaD or SiaD with SiaC at the indicated time-point was determined by HPLC.

Data information: Data represent the means and SDs of three biological replicates. * $P < 0.05$ and ** $P < 0.01$ based on one-way ANOVA test. ns, non-significance. EV represents the empty vector pUCP20 in this and subsequent assays. Source data are available online for this figure.

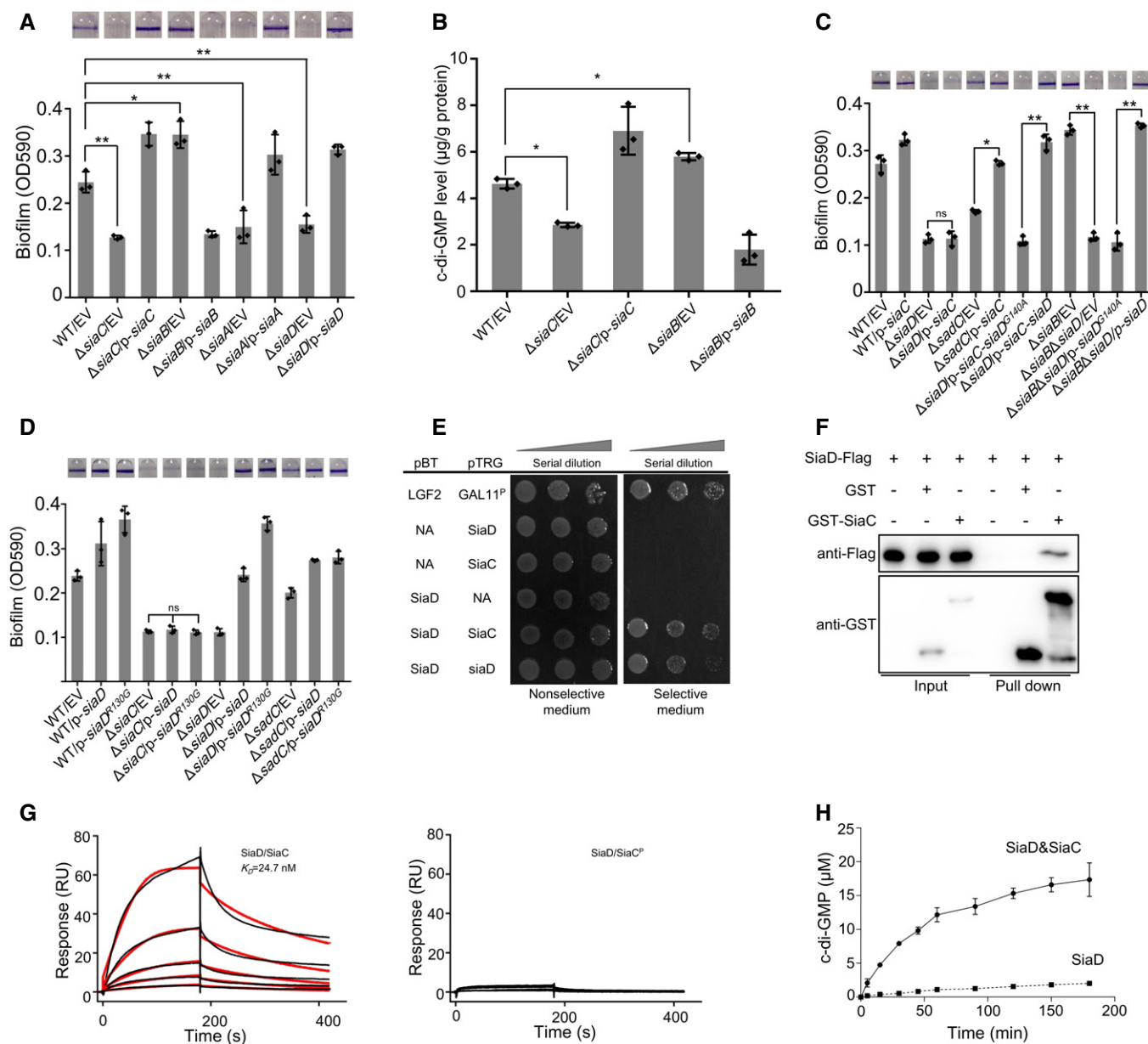


Figure 1.

overexpression of a DGC SadC (for c-di-GMP biosynthesis) in $\Delta siaC$ mutant restored its ability to form biofilm, and the elevated biofilm formation of $\Delta siaB$ was abolished by overexpression of PDE PA2133 (phosphodiesterase, degradation of c-di-GMP) (Appendix Fig S1C). These results suggested that the regulation of biofilm formation by SiaC and SiaB is dependent on the intracellular concentrations of c-di-GMP.

Deletion of *siaD* reduces intracellular c-di-GMP levels (Colley et al, 2016), which regulates biofilm and SDS-induced aggregation. To determine whether the functions of SiaB and SiaC were dependent on SiaD, the abilities to form biofilm of wild-type parent and its derivatives were tested. Overexpression of *siaC* significantly promoted biofilm formation of wild-type parent, whereas this effect was not observed in the $\Delta siaD$ mutant, indicating that the functional SiaD was necessary for the function of SiaC (Fig 1C). Notably,

deletion of another DGC SadC did not abolish the elevated biofilm formation caused by overexpression of SiaC (Fig 1C), suggesting that SiaC-mediated regulation of biofilm formation is specifically dependent on SiaD. To further confirm that SiaC functions by modulating c-di-GMP through SiaD, plasmids overexpressing both *siaC* and *siaD* or *siaD*^{G140A} [a *siaD* active site mutant (Colley et al, 2016)] were constructed and introduced into $\Delta siaD$ mutant, respectively. Biofilm formation assay showed that the elevated biofilm formation by SiaC overexpression was lost in the presence of the *siaD*^{G140A} (Fig 1C). We also revealed that the increased biofilm formation of $\Delta siaB$ was abolished by further deletion of *siaD* gene, which was restored by overexpression of *siaD* but not *siaD*^{G140A} gene (Fig 1C). Together, these results indicated that SiaC and SiaB regulate biofilm and aggregation formation by modulating c-di-GMP levels through SiaD.

SiaC is required for the DGC activity of SiaD via direct interaction

Since the biofilm formation of $\Delta siaC$ is dependent on SiaD, the expression of *siaD* was determined in $\Delta siaC$ mutant. qRT-PCR data showed that deletion of *siaC* reduced the transcript level of *siaD* (Appendix Fig S2A). To determine whether the defect in biofilm formation by $\Delta siaC$ was due to the decreased expression level of *siaD*, plasmid overexpressing SiaD was introduced into $\Delta siaC$. However, our results showed that overexpression of SiaD restored the ability to form biofilm of $\Delta siaD$, but not that of $\Delta siaC$ (Fig 1D). As expected, overexpression of SiaD in $\Delta sadC$ restored the biofilm phenotype (Fig 1D). To confirm that the *siaD* is sufficiently produced from the overexpression plasmid, the plasmid pUCP20-*siaD*-Flag was used to detect the transcription and translation of *siaD*. The function of SiaD was not affected by the C-terminal Flag tag, as the biofilm formation of $\Delta siaD$ was restored after introduction of *siaD*-Flag (Appendix Fig S2B). qRT-PCR and Western blotting results showed that SiaD is sufficiently produced from the overexpression plasmid (Appendix Fig S2C). These results indicated that the function of SiaD is dependent on SiaC.

The failure of overexpressing SiaD to restore the biofilm formation by $\Delta siaC$ prompted us to hypothesize that SiaC directly interacts with SiaD to regulate c-di-GMP production and biofilm formation. To test this, we performed a bacterial two-hybrid (BTH) assay using SiaC as the bait. A specific two-hybrid binding assay using the full-length *siaD* gene construct showed robust growth of colonies on dual-selective medium (Fig 1E), indicating that SiaC interacts with full-length SiaD. The BTH assay suggested that SiaD could interact with itself (Fig 1E), consistent with the finding that GGDEF domains function as homodimers (Romling *et al*, 2013). To further validate the SiaC-SiaD interaction *in vitro*, we performed a GST pull-down assay using the purified GST-SiaC (Appendix Fig S3A) and the lysates of PAO1 cells containing a C-terminal Flag-tagged SiaD plasmid. Western blot analysis showed that SiaD was retained with GST-SiaC, but not GST (Fig 1F). Consistently, a GST pull-down assay using GST-SiaD (Appendix Fig S3A) and SiaC-Flag

demonstrated that GST-SiaD, but not GST, interacts with SiaC-Flag (Appendix Fig S3B). Further, the purified SiaC and SiaD proteins were incubated and the mixtures were subject to analysis by gel filtration chromatography using a Superdex 200 10/300 size exclusion column. Result showed that SiaC forms complexes with SiaD (Fig EV1A). We also performed label-free surface plasmon resonance (SPR) binding assay and found that the purified SiaC binds to SiaD with a dissociation constant (K_D) of 24.7 nM (Fig 1G). However, SiaC was unable to interact with itself (Appendix Fig S3C). Taken together, these results clearly revealed that SiaC directly interacts with SiaD.

The interaction between SiaD and SiaC prompted us to speculate that SiaC acts as a modulator to regulate DGC activity of SiaD. To evaluate the role of SiaC in modulation of the DGC activity of SiaD, enzymatic synthesis of c-di-GMP from GTP was performed *in vitro* using either SiaD or SiaD and SiaC. After incubation, the production of c-di-GMP was analyzed by high-performance liquid chromatography (HPLC) analysis with retention times consistent with those of GTP and c-di-GMP standards. Surprisingly, GTP remained the primary compound in the reaction mix when GTP was incubated with SiaD alone even after 3 h, indicating that SiaD had weak DGC activity (Fig 1H). Interestingly, the production of c-di-GMP was significantly increased when GTP was incubated with both of SiaC and SiaD (Fig 1H), which accounts for the dependence of SiaD on SiaC *in vivo* (Fig 1D). Importantly, SiaC was unable to produce c-di-GMP (Appendix Fig S4A–C) or enhance the activity of another DGC WspR (Appendix Fig S4D–F; Hickman *et al*, 2005). Moreover, our data suggested that the SiaD stability was not influenced by deletion of SiaC (Appendix Fig S2D). Together, these results demonstrated that the direct interaction with SiaC is essential for activation of SiaD DGC activity.

SiaD harbors a conserved RXXD motif (I-site), which is characteristic of c-di-GMP binding and allosteric regulation (Colley *et al*, 2016). Expression of the defective I-site allele *siaD*^{R130G} in $\Delta siaD$ promotes bacterial aggregation compared to a strain complemented with the native *siaD* gene (Colley *et al*, 2016), indicating that I-site mutation abolishes c-di-GMP binding and allosteric regulation.

Figure 2. SiaA and SiaB regulate biofilm formation via interaction with SiaC.

- A Bacterial two-hybrid assay reveals an interaction between SiaB and SiaC. The recombinant strains harboring different proteins were separately streaked on nonselective and dual-selective media (3-amino-1, 2, 4- triazole + streptomycin). NA represents the empty vector pBT or pTRG. The strain-expressing LGF2 and Gal11^P were used as positive controls.
- B Pull-down assays confirmed the interaction between SiaB and SiaC. Cell lysates of *Pseudomonas aeruginosa* containing pMM67EH-*siaC*-Flag were incubated with GST or GST-SiaB individually, and protein complexes were captured by glutathione beads.
- C SPR measurements of SiaC binding at varying concentrations to SiaB. SiaC specifically interacted with SiaB with a K_D of 40.1 nM. Shown are measured binding responses (black) and curve fits to a 1:1 interaction (red). Plots are representative of two experiments with similar results. RU, response units; K_D , dissociation constant.
- D SiaB-mediated regulation of biofilm formation is dependent on SiaC. The biofilm formation of the indicated strains was displayed with crystal violet staining (up) and quantified with optical density measurement (down).
- E Bacterial two-hybrid assay reveals an interaction between SiaC and SiaA PP2C-like domain. NA represents the empty vector pBT or pTRG. The recombinant strains harboring different proteins were separately streaked on nonselective and dual-selective media (3-amino-1, 2, 4- triazole + streptomycin). The strain-expressing LGF2 and Gal11^P were used as positive controls.
- F Pull-down assays confirmed the interaction between SiaC and SiaA. Cell lysates of *Pseudomonas aeruginosa* containing pMM67EH-*siaA*-Flag were incubated with GST or GST-SiaC individually, and protein complexes were captured by glutathione beads.
- G Pull-down assays confirmed the interaction between SiaC and SiaA PP2C-like domain. Cell lysates of *P. aeruginosa* containing pMM67EH-*siaA*₃₈₆-Flag were incubated with GST or GST-SiaC individually, and protein complexes were captured by glutathione beads.
- H The biofilm formation of the indicated strains was displayed with crystal violet staining (up) and quantified with optical density measurement (down).

Data information: Data represent the means and SDs of three biological replicates. ** $P < 0.01$ based on one-way ANOVA test. ns, non-significance. Source data are available online for this figure.

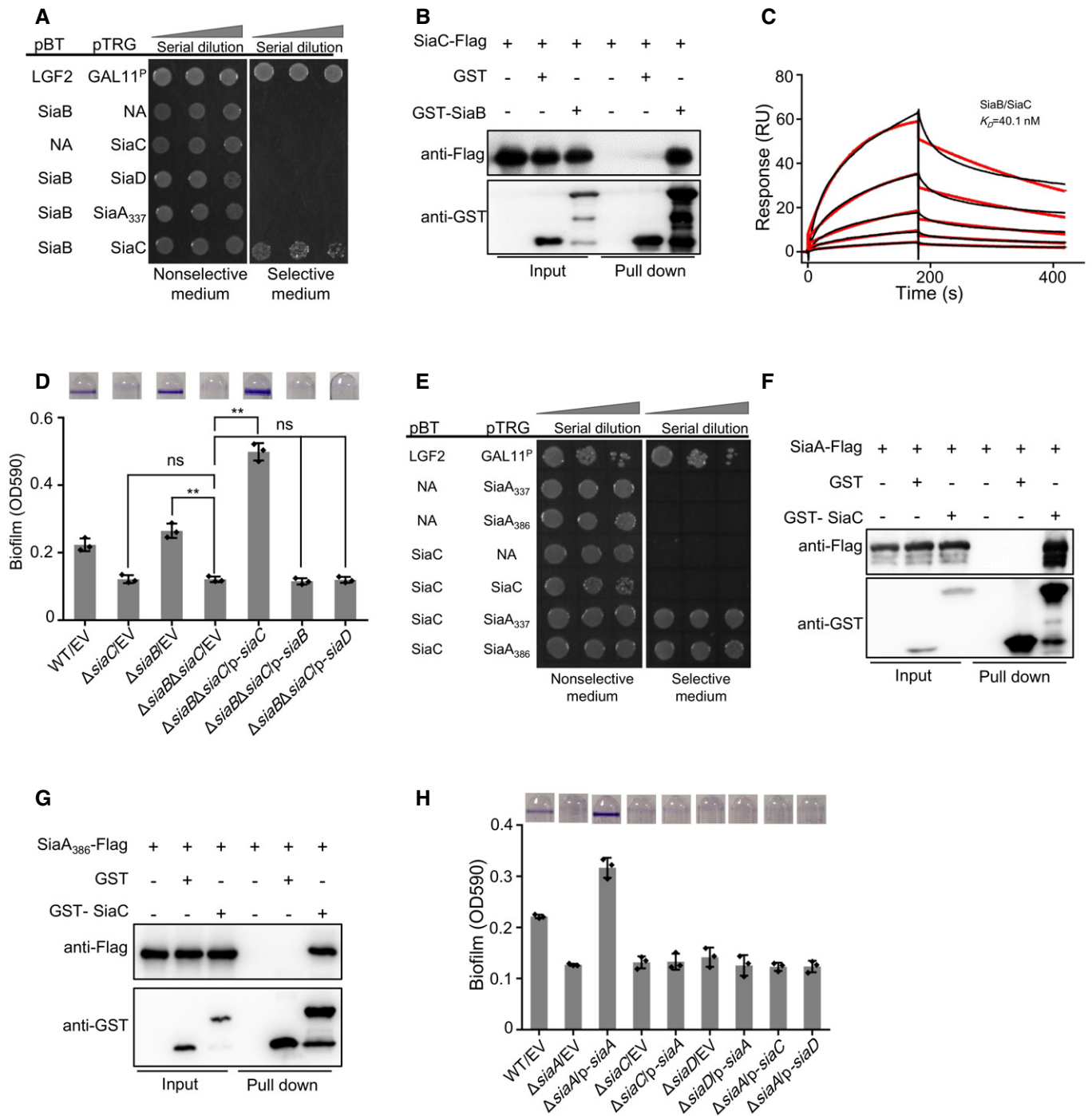


Figure 2.

Therefore, we determined whether SiaC modulates the function of SiaD by repressing c-di-GMP-mediated allosteric regulation. If so, biofilm formation by Δ siaC should be restored by overexpression of $siaD^{R130G}$. However, $siaD^{R130G}$ failed to restore the biofilm-forming ability of Δ siaC (Fig 1D and Appendix Fig S2B). *In vitro* HPLC analysis showed that SiaD^{R130G} has some weak DGC activity, and the activity can be significantly enhanced by SiaC (Appendix Fig S2E). Therefore, SiaC seems unlikely to modulate the function of SiaD by repressing c-di-GMP-mediated allosteric regulation.

SiaB interacts with SiaC to regulate aggregate and biofilm formation

As mentioned above, the hyperbiofilm phenotype of Δ siaB mutant was due to the elevated intracellular c-di-GMP from SiaD (Fig 1C). In addition, SiaC is necessary for the DGC activity of SiaD (Fig 1H). These observations led us to hypothesize that SiaB might interact with SiaC to influence c-di-GMP and biofilm formation. To test this hypothesis, we performed a BTH assay using SiaB as the bait. Like

the positive control, strain-bearing pBT-*siaB* and pTRG-*SiaC* also grew robustly on dual-selective medium (Fig 2A), indicating a direct interaction between *SiaB* and *SiaC*. However, the BTH assay indicated that *SiaB* does not interact with *SiaD* or *SiaA* (Fig 2A). To further confirm the interaction between *SiaB* and *SiaC*, *in vitro* pull-down assays were performed. GST-*SiaB* (Appendix Fig S3A), but not GST, was able to retain *SiaC* (Fig 2B). Consistently, interaction between the purified GST-*SiaC* and *SiaB*-Flag was observed (Fig EV2A). The gel filtration chromatography analysis also indicated the formation of *SiaB*-*SiaC* complex (Fig EV2B). As determined by SPR experiment, *SiaC* can bind to *SiaB* with a K_D of 40.1 nM (Fig 2C). Since both *SiaB* and *SiaD* interact with *SiaC*, we wondered whether the three proteins could form *SiaB*-*SiaC*-*SiaD* ternary complex. However, as confirmed by the pull-down assays, the ternary complex was not formed (Appendix Fig S3D).

To determine whether *SiaC* mediates the function of *SiaB* via direct interaction, we tested the biofilm phenotypes of *P. aeruginosa* and its derivatives. Our results showed that deletion of *siaC* gene in the Δ *siaB* mutant background abolished the hyperbiofilm formation (Fig 2D), suggesting that *SiaB*-mediated biofilm regulation is dependent on its interaction with *SiaC*. As expected, the Δ *siaC* Δ *siaB* double mutant complemented with *SiaB* formed biofilm similar to that of Δ *siaC* (Fig 2D). Additionally, overexpression of *SiaC* in the Δ *siaC* Δ *siaB* double mutant significantly promoted biofilm formation (Fig 2D). However, overexpression of *siaD* did not impact the biofilm phenotype of Δ *siaC* Δ *siaB* strain (Fig 2D). We also determined the SDS-induced aggregation by these strains and similar trends were observed (Appendix Fig S3E). Taken together, these results demonstrated that *SiaC* is essential for *SiaB*-mediated repression of biofilm and aggregates formation.

SiaA regulates biofilm formation via direct interaction with SiaC

SiaA contains two transmembrane helices, PP2C-like phosphatase and HAMP domains (Appendix Fig S5A), which are involved in signal transduction (Aravind & Ponting, 1999; Vijay *et al*, 2000). Deletion of *siaA* reduced biofilm formation, which prompted us to test whether *SiaC* physically interacts with *SiaA*. To determine the protein-protein interaction, and to test whether the HAMP and

C-terminal PP2C-like phosphatase domains are sufficient to maintain the interaction with *SiaC*, we performed specific BTH binding assays using constructs encoding the free-standing PP2C-like phosphatase domain (*SiaA* protein lacking the N-terminal 385 amino acids, *SiaA*₃₈₆) or both the HAMP and PP2C-like phosphatase domains (*SiaA* protein lacking the N-terminal 336 amino acids, *SiaA*₃₃₇). As evidenced by the robust growth of colonies on selective medium (Fig 2E), *SiaC* interacted with the *SiaA* PP2C-like phosphatase domain. To further validate the interaction between *SiaC* and *SiaA*, GST pull-down assays were performed using purified GST-*SiaC* co-incubated with lysate of PAO1 cells containing plasmids expressing Flag-tagged *SiaA* and *SiaA*₃₈₆, respectively. *SiaA*-Flag was shown to be retained with GST-*SiaC* but not GST (Fig 2F). Importantly, *SiaA*₃₈₆-Flag also interacted with GST-*SiaC* (Fig 2G), indicating that *SiaA* interacts with *SiaC* through its PP2C-like phosphatase domain. Notably, we observed no interaction between *SiaD* and *SiaA* (Appendix Fig S5B). Moreover, pull-down assays showed that *SiaA*₃₈₆-*SiaC*-*SiaB* formed a complex, whereas no *SiaA*₃₈₆-*SiaC*-*SiaD* complex was observed (Appendix Fig S5C and D). Taken together, these data indicated that *SiaA* controls biofilm formation and SDS-induced aggregation via direct interaction with *SiaC*.

To assess the functional interplay between *SiaA* and *SiaC*, phenotypic assays were performed. Biofilm assays showed that overexpression of *siaA* restored the ability to form biofilm of Δ *siaA*, but not that of Δ *siaC* or Δ *siaD* (Fig 2H). Surprisingly, overexpression of *siaC* or *siaD* in Δ *siaA* mutant did not promote the biofilm formation, which is in contrast to that observed in wild type (Fig 2H). These results indicated that *SiaA* functions upstream of *SiaC*-*SiaD* and is necessary for their activity. These observations were confirmed by the SDS-induced aggregations of these strains (Appendix Fig S5E). Collectively, these data suggested that *SiaA* is essential for the function of *SiaC* *in vivo*.

Reversible phosphorylation of SiaC by SiaB and SiaA regulates its function

A previous study showed that *SiaC* can be phosphorylated at Thr68 residue (Ravichandran *et al*, 2009). *SiaA* harbors a PP2C-like phosphatase domain, and online homology modeling suggested that *SiaB*

Figure 3. SiaB phosphorylates SiaC at threonine 68 residue and the phosphorylated SiaC is critical for biofilm formation.

- A The relative ATP hydrolysis activity of indicated sample was determined. After ATP hydrolysis reaction, the residual ATP concentration in the reaction buffer was determined by mixing the buffer with luciferase reagent. The emitted light was measured using a microplate luminometer. The amount of ATP hydrolyzed during reaction for each sample represents the ATP hydrolysis activity of each sample. The relative activity of each sample was normalized to that of the sample using *SiaB* and *SiaC*. (–) represents no substrate protein was added to reaction mixture.
- B MS detection of *SiaB* peptide L₆₃LYLNTSSIK₇₂ that was covalently modified with one molecule of phosphate. Extracted ion chromatograms of the doubly protonated peptide are shown with peak intensities indicating the relative amount of either the modified or unmodified peptides.
- C Determination of modification sites by collision-induced dissociation (CID) analysis. The MS/MS spectrum of modified L₆₃LYLNTSSIK₇₂ is shown. The fragment ions b₆ and y₆ to y₉ have a mass increase of 80 corresponding to phosphorylation, suggesting phosphorylation of Thr68.
- D *SiaB* phosphorylates and *SiaA* dephosphorylates *SiaC* *in vitro*. *SiaA* or *SiaA*^{T68A} was added to the reactions containing *SiaB* or *SiaA*₃₈₆ and γ -³²P ATP. Phosphorylated products were separated by SDS-PAGE.
- E Overexpression of *SiaC*^{T68A} restored the ability of Δ *siaA* to form biofilm. The biofilm formation of the indicated strains was displayed with crystal violet staining (up) and quantified with optical density measurement (down).
- F Deletion of *SiaB* in the Δ *siaA* background strain restored the ability of Δ *siaA* to form biofilm. The biofilm formation of the indicated strains was displayed with crystal violet staining (up) and quantified with optical density measurement (down).
- G Production of c-di-GMP at the indicated time-point by *SiaD* with *SiaC* or *SiaC*^{T68A} was determined by HPLC. To evaluate the effect of *SiaB*-mediated phosphorylation on *SiaD* DGC activity, *SiaC* or *SiaC*^{T68A} was pretreated by *SiaB* in the presence of 1 mM ATP before reaction initiation.

Data information: Data represent the means and SDs of three biological replicates. ***P* < 0.01 based on one-way ANOVA test. Source data are available online for this figure.

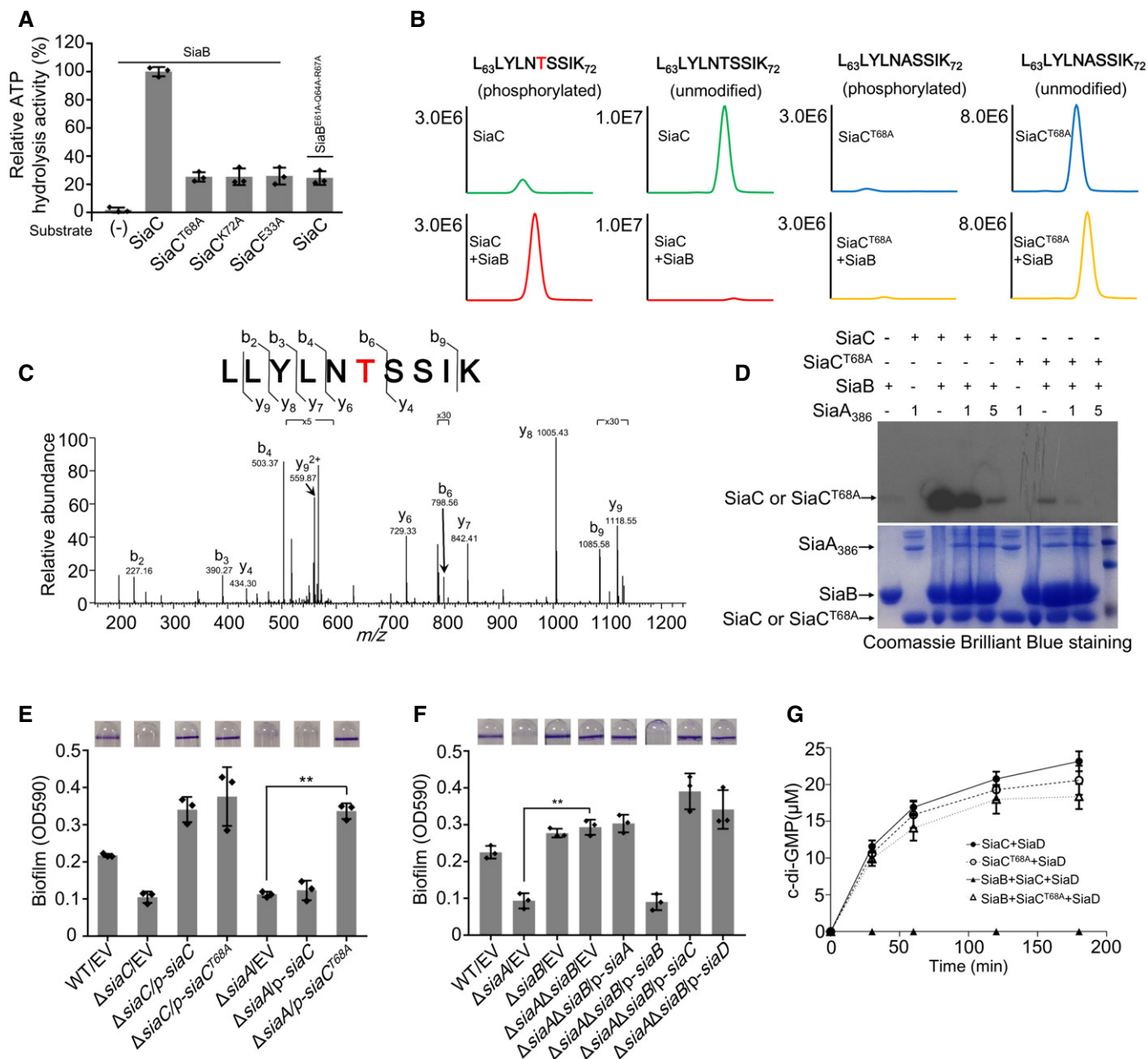


Figure 3.

(Appendix Fig S6A) is similar to alpha-ketoacid dehydrogenase kinase (PDB_ID: 3TZ5) with high confidence (92.1%) (Kelley *et al.*, 2015). This led us to hypothesize that SiaB phosphorylates SiaC, whereas SiaA dephosphorylates it. To test this hypothesis, we assayed ATP hydrolysis activity; SiaB alone exhibited no ATP hydrolysis activity (Fig 3A). However, SiaB displayed ATP hydrolysis activity when purified SiaC was used as the substrate (Fig 3A). The activity of SiaB was independent of the presence of divalent cations, such as Mg^{2+} and Mn^{2+} , as SiaB hydrolyzed ATP in the presence of ethylene diamine tetraacetic acid (EDTA; Appendix Fig S6B).

Mass spectrometric analysis of SiaC *in vitro* in the presence of SiaB kinase confirmed the phosphorylation site at Thr68 (Fig 3B and C, and Table EV1), indicating that SiaB phosphorylates SiaC. Indeed, quantitative radioactive phosphorylation assays verified

that SiaC was specifically phosphorylated by SiaB (Fig 3D). Next, we assessed the ability of SiaA to dephosphorylate SiaC. Because the expression and purification of full-length SiaA is problematic, a truncated protein containing only the C-terminal phosphatase domain of SiaA (SiaA₃₈₆) was used. When present at sub-stoichiometric ratios to SiaB, SiaA significantly decreased the level of phosphorylated SiaC (Fig 3D). SPR data showed that purified SiaC or SiaC^P binds to SiaA₃₈₆ with a K_D of 19.2 nM or 46.5 nM (Fig EV2C), demonstrating slight difference for SiaA₃₈₆-SiaC and SiaA₃₈₆-SiaC^P binding. The interaction between SiaC^P and SiaA₃₈₆ was also confirmed by pull-down assays (Fig EV2D) in the presence of Mg^{2+} . These data suggest that SiaA has protein phosphatase activity and dephosphorylates SiaC at the site phosphorylated by SiaB.

Because $\Delta siaA$ was deficient in biofilm formation, whereas $\Delta siaB$ exhibited enhanced biofilm formation, we speculated that the reversible phosphorylation of SiaC by SiaB and SiaA regulates the DGC activity of SiaD. To test this hypothesis, a strain with the point mutation T68A (Thr 68 to Ala) was tested for its ability to complement biofilm and aggregate formation by $\Delta siaC$ and $\Delta siaA$. In contrast to wild-type SiaC, SiaC^{T68A} restored the ability of $\Delta siaA$ to form biofilm and aggregates (Fig 3E and Appendix Fig S6C). *In vitro* GST pull-down assay revealed that purified SiaC^{T68A} was able to interact with GST-SiaB (Fig EV2E). In addition to T68A, we also constructed a T68D mutant. Like T68A mutant, overexpression of SiaC^{T68D} also restored the biofilm formation of $\Delta siaA$ and $\Delta siaC$ (Appendix Fig S6D). This result indicated that phosphorylation of SiaC by SiaB inhibits SiaC to promote biofilm formation *in vivo*. Next, to confirm the effect of SiaB on biofilm formation, we created a $\Delta siaA\Delta siaB$ double mutant. Although $\Delta siaA$ was deficient in biofilm formation, further deletion of *siaB* ($\Delta siaA\Delta siaB$) significantly promoted biofilm formation, similar to $\Delta siaB$ (Fig 3F). Furthermore, HPLC was performed to evaluate the effect of SiaC phosphorylation on the activity of SiaD. Purified SiaC and SiaC^{T68A} were pre-incubated with SiaB before being added to the DGC reaction mixture. Pre-incubation with SiaB rendered SiaC unable to promote the activity of SiaD (Fig 3G). However, the function of SiaC^{T68A} was not influenced by SiaB (Fig 3G). Unlike native SiaC, both SPR and pull-down assays revealed that SiaC^P was unable to interact with SiaD (Figs 1G and EV1B). Taken together, these results provide strong evidence that SiaC is a physiological substrate for SiaB and SiaA. Furthermore, the antagonistic activity of SiaB and SiaA at Thr68 of SiaC modulates the function of that protein.

Overall structure of SiaB/SiaC complex

To understand the underlying basis for SiaC binding and phosphorylation by SiaB, we carried out crystallization studies. After extensively screening, we successfully obtained the crystals and solved the SiaB/SiaC complex structure at high resolution (2.1 Å, Appendix Table S1). The crystal belongs to P2₁ space group. The asymmetric unit contains four protein molecules, including two SiaB and two SiaC, assembled into a “II” shape (Fig 4A). The two SiaB molecules exist as dimer (Appendix Fig S7), forming the top of the architecture, whereas the sides are formed by the two SiaC molecules. Both SiaB and SiaC are of α/β -fold in nature (Fig EV3A and B). SiaB is composed of six α -helices and five all anti-parallel β -sheets. The β -strands form one flat β -sheet, packed against $\alpha 4$ helix on one side. Conformations of the β -sheet and $\alpha 4$ are stabilized by packing with helices $\alpha 2$, $\alpha 3$, $\alpha 5$, and $\alpha 6$. SiaC is composed of three

α -helices and six β -strands. Except $\beta 2$, the other five β -strands are parallel to each other. Like SiaB, the β -strands of SiaC also form one flat β -sheet, which packed against helices $\alpha 1$ – $\alpha 3$ on the same side.

The interactions between SiaB and SiaC are mainly mediated by the helices of SiaB (Fig EV3C) and the loops of SiaC (Fig EV3D). As depicted in Fig 4B, the side chain of Glu32 of SiaB forms two direct hydrogen bond (H-bond) interactions with Gln10 and Ser11 of SiaC. Bridged one water molecule, the main chain of Glu32 of SiaB interacts with Tyr31 of SiaC, which further forms one H-bond interaction with Gln64 of SiaB. Direct H-bond interactions are also formed between the side chains of Glu61 and Gln64 of SiaB and Tyr65 and Asn67 of SiaC (Fig 4B). The SiaB/SiaC complex formation is further stabilized by three pairs of salt-bridges, formed between Asp54, Arg67, and Arg154 of SiaB and Arg103, Glu33, and Glu110 of SiaC, respectively (Fig 4B).

To confirm their involvement in the formation of the SiaB-SiaC complex, we performed a mutational analysis of a subset of these residues (E32A, E61A, Q64A, E61A-Q64A, E61A-Q64A-R67A for SiaB and, E33A, R103A, E110A for SiaC) in a quantitative biofilm assay. We observed that the mutant SiaC^{E33A} restored the ability of $\Delta siaA$ to form biofilm, which suggested that Glu33 of SiaC is important for the phosphorylation of SiaC by SiaB (Fig 4C). Additionally, although none of the single mutations abolished the function of SiaB *in vivo*, the SiaB^{E61A-Q64A-R67A} triple mutant failed to restore the ability of $\Delta siaB$ to form biofilm to the level of the wild-type strain (Fig 4D). Western blot analysis showed that the E61A-Q64A-R67A triple mutation did not influence SiaB expression (Appendix Fig S8). Consistently, the E61A-Q64A-R67A (SiaB) and E33A (SiaC) mutations significantly reduced the kinase activity of SiaC (Fig 3A). According to these data, the residues implicated in the formation of the SiaB-SiaC complex are essential for the kinase activity of SiaB *in vivo*.

Basis for cofactor binding and phosphorylation

During the crystallization process of SiaB/SiaC complex, cofactor ATP was included in the protein sample. As supported by the clear electron density maps (Fig 5A), the phosphorylation reaction occurred, transforming ATP molecule into ADP. The nucleobase of ADP is bound in one deep pocket of SiaB (Fig 5B). The conformation of ADP nucleobase is stabilized by several different types of interactions (Fig 5C), including the direct H-bond interaction between ADP N1 atom and the ND2 atom of Asn100, water-mediated H-bond interactions with the main chain of Met62 and side chain of Asn65, and hydrophobic stacking interactions with the side chains of Tyr69 and Leu110. The conformation of

Figure 4. The complex structure of SiaB/SiaC.

- The overall fold of SiaB/SiaC complex. The two SiaB molecules are shown as cartoons in light blue and pink, respectively. The two SiaC molecules are all shown as cartoons in yellow. ADP and TPO68 are shown as spheres in atomic colors (C, cyan; N, blue; O, red; P, orange).
- Detailed interactions between SiaB and SiaC. The interacting residues are showing as sticks. The C-atoms of SiaB and SiaC residues are colored in light blue and yellow, respectively. H-bonds are indicated by black dashed lines.
- SiaC^{E33A} partially restored the biofilm formation of $\Delta siaA$. The biofilm formation by the indicated strains was displayed with crystal violet staining (up) and quantified with optical density measurement (down).
- Triple mutation of E61A-Q64A-R67A is important for the function of SiaB. The biofilm formation by the indicated strains was displayed with crystal violet staining (up) and quantified with optical density measurement (down).

Data information: Data represent the means and SDs of three biological replicates. ** $P < 0.01$ based on one-way ANOVA test.

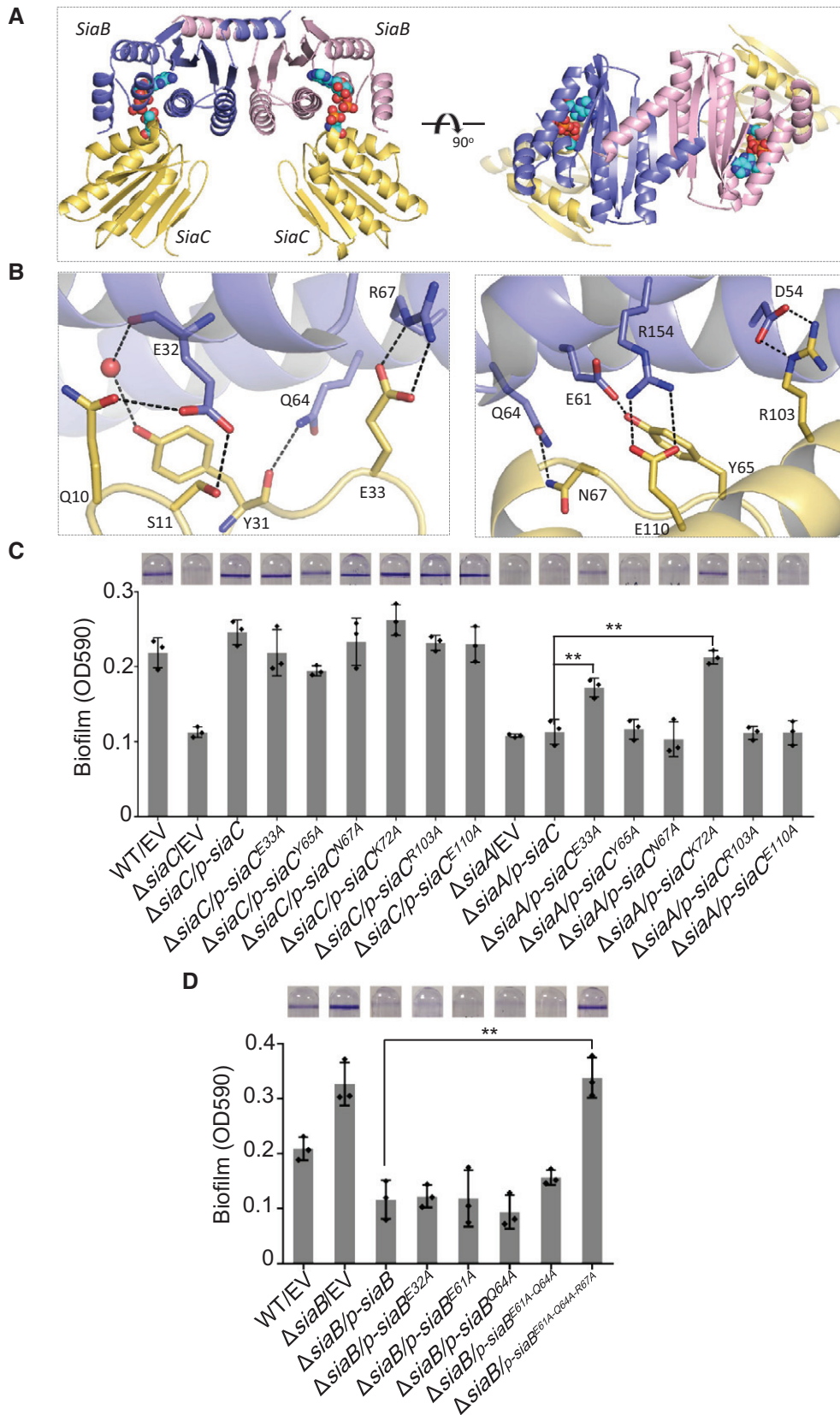


Figure 4.

Leu110 is in turn stabilized by Phe174. The two phosphate groups of ADP sit next to the N-terminus of $\alpha 6$ helix of SiaB, forming two H-bonds [one between the O2A atom of ADP and

the N atom of Leu149 and the another between the O2B atom of ADP and the N atom of Gly148 (Fig 5D)]. SiaB could bind to unphosphorylated SiaC (Fig 2C); however, SPR and pull-down

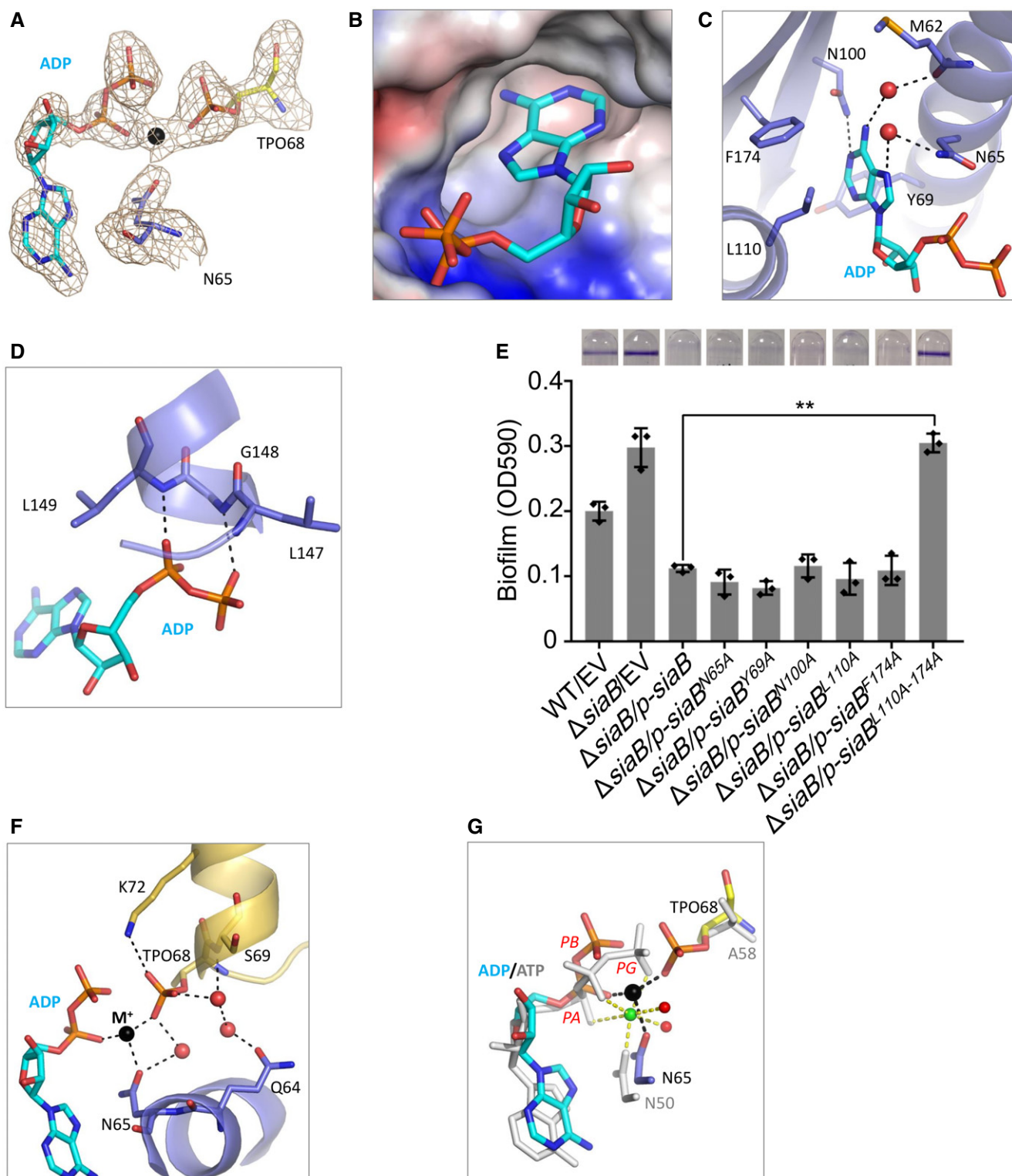


Figure 5.

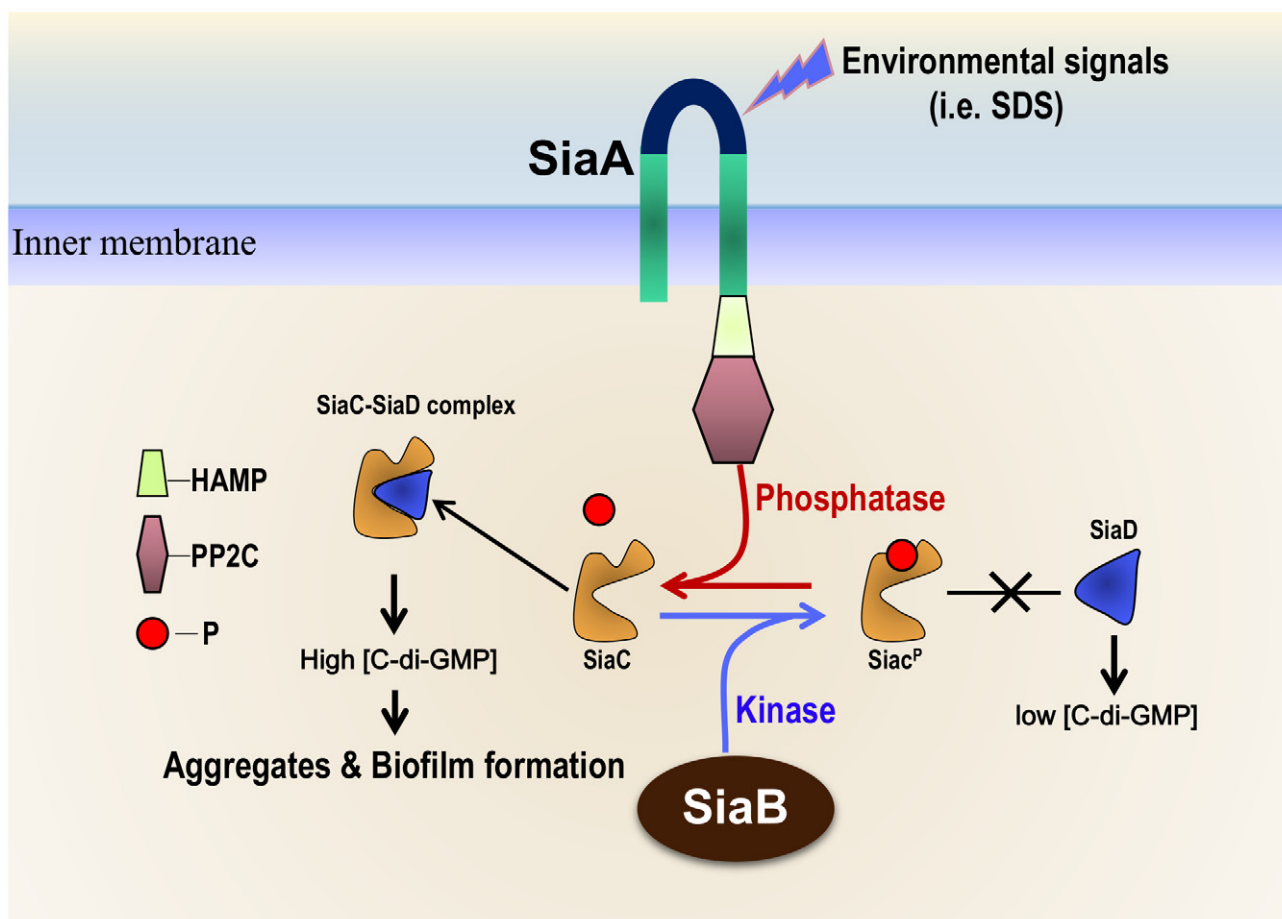
Figure 5. ADP binding and phosphorylation.

- A $F_o - F_c$ omit map of ADP and TPO68. The map was contoured at 2.5 σ level. ADP, TPO68 of SaiC, and Asn65 of SiaB are shown as sticks. Na⁺ ion is shown as black sphere.
- B Surface presentation of the ADP binding pocket.
- C Detailed interactions between ADP and SiaB. ADP and the interacting residues are shown as sticks.
- D Interactions between ADP and residues Leu149 and Gly148. ADP and the interacting residues are shown as sticks.
- E Leu110 and Phe174 residues are important for SiaB function. The biofilm formation by the indicated strains was displayed with crystal violet staining (up) and quantified with optical density measurement (down). Data represent the means and SDs of three biological replicates. **** $P < 0.01$** based on one-way ANOVA test.
- F Conformation of TPO68 and coordination of Na⁺ ion. Na⁺ ion and water molecules are shown as spheres in black and red, respectively.
- G Comparison of the cofactors bound at the active sites of SiaB/SiaC and BsSpoIIAB/SpoIIAA complexes. For SiaB/SiaC complex, ADP, TPO68 of SaiC, and Asn65 of SiaB are all shown as sticks in atomic colors (O, red; N, blue), whereas their C-atoms are colored in cyan, yellow, and light blue, respectively. For BsSpoIIAB/SpoIIAA complex, ATP, Ala58 (mutation of Ser58) of SpoIIAA, and Asn50 of SpoIIAB are all colored in white. Mg²⁺ ion and its coordinating water molecules are shown as spheres in green and red, respectively.

results showed that SiaB was unable to bind to SiaC^P in the absence of ADP (Fig EV4A and B). We failed to purify protein SiaB^{L110A-F174A} or detect its kinase activity due to the insolubility of this protein when expressed in *Escherichia coli*. However, a biofilm formation assay using SiaB mutants showed that the L110A-F174A double mutation abolished its function (Fig 5E).

Compared to SiaB-Flag, the expression level of SiaB^{L110-F174A}-Flag was lower during biofilm formation (Appendix Fig S8). Altogether, these results indicated that the residues Leu110 and Phe174 are important for the function of SiaB.

Thr68 of SiaC is the targeting residue of SiaB. In the complex structure (Fig 5F), Thr68 has been phosphorylated and was termed

**Figure 6. Proposed model of the SiaABCD signaling network involved in regulation of biofilm and aggregate formation.**

Under normal conditions (such as in rich media), the protein kinase SiaB dominates and maintains most SiaC phosphorylated, which failed to bind to SiaD or induce the DGC activity of SiaD; therefore, c-di-GMP is insufficient to activate the biofilm and aggregate formation. Once under stress conditions (such as SDS stimulation), SiaA phosphatase is activated and most SiaC stays unphosphorylated; in this situation, the unphosphorylated SiaC promotes the DGC activity of SiaD and produces sufficient c-di-GMP, which leads to aggregate and biofilm formation.

as TPO68 hereafter. The phosphate group of TPO68 forms one H-bond interaction with the side chain NZ atom of Lys72 of SiaC. Via one water molecules, the TPO68 phosphate group interacts with the main chain N atom of Ser69 of SiaC. Water-mediated interactions are also formed between TPO68 phosphate group and the side chains of Gln64 and Asn65 of SiaB. The structural data suggested that Lys72 of SiaC may play an important role in SiaC phosphorylation. To further confirm this observation, we performed biofilm assay and found that SiaC^{K72A} restores the ability of Δ siaA to form biofilm, indicating that the mutated protein is present *in vivo* predominantly in the unphosphorylated state (Fig 4C). Additionally, the ATP hydrolysis activity of SiaB was significantly impaired when SiaC^{K72A} was used as the substrate (Fig 3A). In addition to ADP, one well-defined metal ion was observed in the complex and coordinated with the O1A atom of ADP, the O2P atom of TPO68, and the OD1 atom of Asn65 of SaiB. Through sample and crystallization condition analysis, we speculated that this was likely to be a Na⁺ ion captured in the structure. Notably, our ATP hydrolysis assay showed that SiaB is still active in the ammonium phosphate buffer without Na⁺ (Appendix Fig S6E), suggesting that Na⁺ ion is not strictly required for the ATP hydrolysis activity of SiaB. However, cations (Na⁺, NH₄⁺, or others) could still play certain role in the function of SiaB, such as stabilizing the SiaB-SiaC complex.

Dali search program showed that SiaB shares similar fold with some kinase proteins. The two closest matches, SpoIIAB from *Bacillus stearothermophilus* (Masuda *et al*, 2004) and SpoIIAB from *Bacillus subtilis* (Campbell *et al*, 2002), all gave a Z-score of 11.5. The root mean square deviation (rmsd) values between SiaB and the two SpoIIAB proteins are around 2.8 Å. However, the overall sequence similarities between SiaB and SpoIIAB proteins are very low (< 10%). As depicted in Fig EV5A, SiaB can superimpose with BsSpoIIAB at the β -strand, α 2, α 3, and α 6 regions, whereas it is very different from BsSpoIIAB at α 1, α 4, and α 5 regions. α 1 is involved in dimerization of SiaB (Appendix Fig S7), but it is absent in SpoIIAB proteins. Instead of α -helices, the region corresponding to α 4 and α 5 of SiaB folds into one short α -turn followed by one extended loop in BsSpoIIAB (Fig EV5B). The loop was termed as ATP-lid previously; it contains one conserved arginine residue, which interacts with the γ -phosphate and stabilizes the conformation of ATP in the BsSpoIIAB/SpoIIAA complex structure. SpoIIAB can catalyze the phosphorylation of a Ser residue of SpoIIAA. BsSpoIIAB/SpoIIAA and our SiaB/SiaC structures represent the reaction states prior to and after phosphorylation, respectively. The orientations of the nucleobases of ADP in SiaB/SiaC complex and ATP in the BsSpoIIAB/SpoIIAA complex are very similar (Fig 5G). In the BsSpoIIAB/SpoIIAA complex, one Mg²⁺ was captured. In addition to ATP, the Mg²⁺ ion also coordinates with the side chain of Asn50. Asn50 of BsSpoIIAB corresponds to Asn65 of SiaB, and they adopt similar conformations in the two structures. Owing to the different reaction states, the conformations of the phosphate groups are slightly different. However, the relative orientations between ATP (or ADP) and the targeting residues (Thr or Ser) are similar, suggesting that SiaB and BsSpoIIAB may follow a similar mechanism in catalysis.

Besides SiaB/SiaC complex, one apo-SiaC structure was also solved in this study (Appendix Table S1). Indicated by the very low rmsd value (0.3 Å), the overall conformations of SiaC are

virtually identical in the complex and apo-structures. However, structural superposition could reveal some conformational changes of SiaC, especially at residue 102–104 region (Fig EV5C). Arg103 of SiaC is involved in the binding with SiaB (Fig 4B). Both Glu102 and Arg103 are disordered in the apo-structure, whereas they fold into the N-terminus of α 3 in the complex structure. Interestingly, superposition also revealed some structural similarity between SiaC and BsSpoIIAA, especially at their β -sheet and α 2 region (Fig EV5D). The rmsd value between SiaC and BsSpoIIAA is 2.9 Å and the Dali search Z-score between the two proteins is 7.9. As described above, the phosphate group of TPO68 interacts with Lys72 of SiaC in SiaB/SiaC complex structure. However, such lysine residue is not present in BsSpoIIAA. Taken together, these results demonstrate that SiaB is a unique kinase that plays an important role for the activity of SiaC.

Discussion

The putative Ser/Thr phosphatase SiaA and the regulation of the c-di-GMP level by SiaD have been proposed to modulate sodium dodecyl sulfate-induced macroscopic aggregation (Klebensberger *et al*, 2009). We report here that the direct interactions among SiaD, SiaC, SiaB, and SiaA constitute a signaling network that regulates biofilm formation by modulating the intracellular c-di-GMP level. Within this network, the direct interaction of SiaC with SiaD regulates the DGC activity of the latter, which increases c-di-GMP production and biofilm formation. Furthermore, the biochemical and structural data revealed that SiaB is a kinase with several unique characteristics. Both SiaB and the phosphatase SiaA reverse-phosphorylate SiaC, which is important for regulating the DGC activity of SiaD. Based on our data, we propose a model in which SiaC plays a central role via its interactions with the other three proteins (Fig 6). Under normal conditions (such as in rich media), the kinase SiaB maintains SiaC phosphorylation, preventing SiaC-SiaD interaction, hampering activation of the DGC activity of SiaD. Under stress conditions (such as sodium dodecyl sulfate, SDS), SiaA phosphatase is activated by an unknown signal and most SiaC remains unphosphorylated, leading to SiaD activation and c-di-GMP production, thus promoting the formation of aggregates and biofilm. In addition, the extensive distribution of homologues of these proteins among bacterial taxa suggests the importance of this system (Appendix Fig S9).

SiaC seems to be a key player in the signaling pathway. SiaD alone exhibited weak DGC activity (Fig 1H), consistent with a previous report of the lack of c-di-GMP in an extract of a *siaD*-overexpressing strain (Kulasakara *et al*, 2006). Additionally, direct interaction of SiaC with SiaD regulates the DGC activity of the latter, consistent with the observation *in vivo* that *siaC* is required for the SiaD-mediated promotion of biofilm formation (Fig 1D). In *P. aeruginosa*, the DGC WspR is activated by phosphorylation and the activity of SadC is controlled by its transmembrane domain and the presence of oxygen (Hickman *et al*, 2005; Schmidt *et al*, 2016; Zhu *et al*, 2016a). Post-translational modulation of the activity of SiaD by its direct interaction with SiaC is in agreement with these reports. However, it is unlikely that direct interaction with SiaC stabilizes SiaD or represses the allosteric inhibition by c-di-GMP (Appendix Fig S2D and Fig 1D). The mechanism by which the

interaction between SiaC and SiaD regulates the DGC activity of the latter is unclear. The SiaD-SiaC interaction may alter the conformation of SiaD to promote its binding to GTP, thus producing c-di-GMP. Further studies of the underlying molecular mechanisms are needed.

Protein phosphorylation is a ubiquitous regulatory mechanism that affects multiple cellular processes (Hunter, 1995; Taylor & Kornev, 2011). During surface-bound growth of *P. aeruginosa*, the hybrid response regulator/DGC, WspR, is activated via phosphorylation by the Wsp chemosensory system (Hickman et al, 2005; Guvener & Harwood, 2007). Activation of DGC HsbD in *P. aeruginosa* (Valentini et al, 2016) and BgrR in *Sinorhizobium meliloti* (Baena et al, 2019) is accomplished via phosphorylation by the individual binding partner. In this study, we revealed a similar signaling network for modulation of SiaD activity. Given the wide distribution of homologues of SiaC (Appendix Fig S9), the activation model for DGC revealed here should be universal among bacteria.

SiaC is modified post-translationally by the SiaB kinase and SiaA phosphatase. No interaction between SiaB and SiaD was observed (Fig 2A); therefore, SiaB cannot directly modify SiaD. Additionally, because the GST pull-down data showed that SiaB can interact with SiaC^{T68A} (Fig EV2E), it seems unlikely that SiaB prevents the activation of SiaD by sequestering SiaC. Several lines of evidence indicate that reversible phosphorylation of SiaC by SiaB and SiaA is essential for the modulation of SiaD DGC activity. First, the Δ siaA mutant was deficient in biofilm formation, including in the presence of a plasmid overexpressing *siaC* or *siaD*, whereas further deletion of SiaB (Δ siaA Δ siaB) significantly promoted biofilm formation (Fig 3F). Second, overexpression of SiaC restored the ability of Δ siaA to form biofilm when the target residue of phosphorylation, Thr68, was substituted for alanine (Fig 3E). Third, phosphorylated SiaC was unable to interact with SiaD (Figs 1G and EV1B). Finally, HPLC showed that pre-incubation with the kinase SiaB inhibits the promotion of the DGC activity of SiaD by SiaC, whereas the function of SiaC^{T68A} was not affected by SiaB (Fig 3G). Moreover, we solved the crystal structure of SiaB/SiaC complex, demonstrating SiaB is a kinase and can phosphorylate the Thr68 residue of SiaC. Consistently, the mass spectrometric quantitative radioactive phosphorylation assays showed that the kinase SiaB specifically phosphorylates SiaC. Though SiaB shares some similarities in folding and catalytic mechanism with other protein kinases, it possesses some very unique structural features, especially at the ATP binding region. Many protein kinases contain an ATP-lid loop, which is flexible and can undergo large conformational changes upon the binding (or dissociation) of cofactor ATP (or ADP), whereas SiaB has two rigid helices (α 4 and α 5) surrounding the ATP binding region. Compared to other kinases, SiaB lacks the ATP-interacting Arg residue within the loop region. However, our structure and *in vitro* data suggested that Lys72 of SiaC plays a critical role in the SiaB-catalyzed phosphorylation reaction. Taken together, we conclude that SiaB is a unique kinase and it may follow a substrate-mediated mechanism in catalysis.

SiaA harbors a PP2C-like phosphatase domain, a typical output domain in bacterial transmembrane receptors that respond to energy stress, such as RsbP of *B. subtilis* (Vijay et al, 2000). SiaA and SiaD might respond to the extracellular polysaccharide Psl in mixed-species biofilms (Irie et al, 2012; Chew

et al, 2018). However, overexpression of SiaC or SiaA in the Δ pslBCD mutant displays the similar biofilm phenotype as the wild-type parent, indicating activation of SiaD by SiaC *in vivo* is independent on the polysaccharide Psl, at least in the present experiment conditions (Appendix Fig S10). The direct interaction between SiaC and the PP2C-like domain of SiaA and the results of radioactive phosphorylation assays suggest that SiaC is the downstream target of SiaA. Because SiaA is essential for SiaC-mediated promotion of the formation of biofilm and aggregates, dephosphorylation by SiaA should be important for the activation of SiaD by SiaC.

In conclusion, we identified a novel signaling network that regulates biofilm formation by modulating the activity of SiaD and the intracellular level of c-di-GMP, wherein SiaC switches the DGC activity of SiaD “on” and “off” after receiving an upstream signal from SiaB or SiaA. *P. aeruginosa* may use this signaling network to rapidly respond and adapt to environmental changes.

Materials and Methods

Bacterial strains and culture conditions

Bacterial strains, plasmids, and primers used are listed in Appendix Tables S2 and S3. Strains were incubated in LB medium or M9 salt (6.78 g/l Na₂HPO₄, 3 g/l KH₂PO₄, 0.5 g/l NaCl, 1.0 g/l NH₄Cl) with succinate (10 mM) or SDS (0.1%) as the sole carbon source. When needed, appropriate antibiotics were supplemented: tetracycline (100 μ g/ml) and carbenicillin (150 μ g/ml) for *P. aeruginosa*, and tetracycline (20 μ g/ml) and carbenicillin (100 μ g/ml) for *E. coli* (Sangon life sciences).

Plasmids construction

To construct mini-CTX-*lacZ*-*siaD*-Flag plasmid, the DNA fragments containing *siaA* promoter, *siaD* coding region, and Flag-tag encoding sequence were generated by overlap PCR using mini-*siaD*-F1/R1 and mini-*siaD*-F2/R2 primer pairs. The DNA fragments were then cloned into mini-CTX-*lacZ* vector (Becher & Schweizer, 2000). The purified PCR products amplified by pUC-*siaD*-F/pUC-*siaD*-R primer pair were digested with *Bam*H1 and *Hind*III enzymes and cloned into pUCP20 plasmid (West et al, 1994), yielding pUC-*siaD* plasmid. Plasmids pUCP-*siaA*, pUCP-*siaC*, and pUCP-*siaB* were constructed similarly. The pMMB67EH-Flag vector was constructed based on pMMB67EH to overexpress Flag-tagged genes. Vector pMMB67EH was digested with *Hind*III before blunted by T4 DNA polymerase (Transgene, Beijing, China). The blunted fragment was then digested with *Pst*I enzyme. DNA fragments containing Flag tag coding sequence were amplified by primers flag-up and flag-dn, digested with *Pst*I and *Eco*RV and cloned into the *Pst*I-digested pMMB67EH. For construction of pMMB67EH-*siaD*-Flag plasmid, the purified PCR products amplified by pMM-*siaD*-F/pMM-*siaD*-R were digested with *Bam*H1 and *Sal*I enzymes and cloned into the *Bam*H1-*Xho*I digested pMMB67EH-Flag plasmid fragment. Accordingly, the coding sequences of *siaC*, *siaB*, *siaA*, *siaA*₃₃₇, and *siaA*₃₈₆ were amplified with the corresponding primer pairs and cloned into the pMMB67EH-Flag vector after enzymatic digestion.

Construction of *Pseudomonas aeruginosa* deletion mutants

In-frame deletion mutants were generated as described previously (Hoang *et al.*, 1998). To construct the *siaC* deletion mutant, PCRs were performed to amplify sequences upstream (1,724) and downstream (1,499) of the intended deletion with primer pairs *siaC*-H1F/H1R and *siaC*-H2F/H2R. The homologous arms were digested and cloned into *EcoRI*/*HindIII*-digested vector pEX18Tc, yielding pEX-*siaC*. The resulting plasmid was transformed into PAO1 with selection for tetracycline-resistant first homologous recombinants. Colonies were then streaked on LB agar plates with 10% sucrose to select second homologous recombinants. And the Δ *siaC* mutant was identified by PCR using primers *siaC*-H1F and *siaC*-H2R. For generating Δ *siaA*, Δ *siaD*, Δ *siaB*, Δ *siaC* Δ *siaB* deletion mutants, similar strategy was applied. All resultant mutants were verified by PCR and DNA sequencing.

Biofilm formation assay

Biofilm formation assay was performed as described previously with modification (Zhu *et al.*, 2016b). Briefly, overnight cultures grown in LB medium were diluted (1:1,000) into 1-ml fresh LB medium in glass tube and incubated statically at 25°C for 22 h. Biofilms attached to the sides of the glass tubes were washed twice gently with sterile water and stained with crystal violet (CV). Quantification of biofilm biomass was performed by dissolution of the CV-stained biofilm with ethanol, and the CV solution was measured at an absorbance of OD₅₉₀ nm. The assay was performed at least three times with a minimum of three replicates for each strain.

SDS-induced macroscopic aggregation

Macroscopic aggregation was performed as previously described with slight modification (Klebensberger *et al.*, 2009). Briefly, overnight cultures of bacterial strains were diluted (1:100) into 2 ml fresh M9 salt with 10 mM succinate or 0.1% SDS as sole carbon source. Macroscopic aggregation was tested after 12-h growth in glass tubes on a rotary shaker at 180 rpm at 37°C. The aggregations were gently transferred into 24-well plate for photographing.

RNA extraction and real-time quantitative PCR

Overnight bacterial cultures were sub-cultured in fresh LB medium until stationary phase (OD₆₀₀ = 2.0). The bacterial strains were collected by centrifugation at 12,000 g for 2 min. Total RNA was isolated with RNeasy pure cell/bacteria kit (Qiagen Biotech, Beijing, China). cDNA was synthesized from each RNA sample using a PrimerScript Reverse Transcriptase (Takara, Dalian, China) with random primer, then subjected to qRT-PCR using SYBR Premix Ex Taq II (Takara). The 30s ribosomal protein gene *rpsL* was used as an internal control.

Bacterial two-hybrid experiments

The bacterial two-hybrid assays were performed as previously described (Zhao *et al.*, 2016). Briefly, the bait and prey plasmids were co-transformed into *E. coli* reporter strain before plated onto selective and nonselective media. After grown on M9 + His-deficient

medium containing 5 mM 3-amino-1,2,4-triazole (3-AT) for 24–48 h at 30°C, colonies appeared on these plates were selected. Positive colonies were streaked on M9⁺ His-deficient medium containing 5 mM 3-AT and 12.5 μg/ml streptomycin and subject to gradient dilution and plate inoculation.

Protein purification

To purify GST-SiaA₃₈₆, GST-SiaB, GST-SiaC, and GST-SiaD, the pGEX6p-*siaA*₃₈₆, pGEX6p-1-*siaB*, pGEX6p-1-*siaC*, or pGEX6p-1-*siaD* was transformed into *E. coli* BL21 (DE3), respectively. Bacteria were cultured at 37°C in LB medium to an OD₆₀₀ of ~ 0.6 before shifted to 16°C and induced with 0.5 mM IPTG and then cultivated for an additional 20 h at 16°C. Harvested cells were resuspended in GST buffer A (50 mM Tris-HCl, pH 8.0 150 mM NaCl) and sonicated, and proteins were purified with the 5-ml GSTrap HP column (GE Healthcare) using GST buffer B (50 mM Tris-HCl, pH 8.0 150 mM NaCl, 10 mM glutathione). For purification of Sumo-SiaD, Sumo-SiaD^{R130G}, Sumo-SiaC, and Sumo-SiaB proteins, the corresponding plasmid was constructed and proteins were purified with 5-ml HisTrap HP column (GE Healthcare, USA) using His buffer A (10 mM Tris-HCl, pH 8.0, 500 mM NaCl, 1 mM DTT) and His buffer B (10 mM Tris-HCl, pH 8.0, 500 mM NaCl, 1 mM DTT, 500 mM imidazole) according to manufacture's instructions. The purified proteins were then digested by UlpI protease to remove the Sumo. For size exclusion chromatography, the purified Sumo-SiaD and Sumo-SiaC or Sumo-SiaB and Sumo-SiaC were mixed for 1 h before UlpI protease digestion. The samples were loaded onto a Ni-NTA resin column again, and the flow-through containing the target proteins was collected. The samples were concentrated and passed through a 10/300 Superdex 200 size exclusion column (GE Healthcare, USA) equilibrated with SEC buffer (10 mM Tris-HCl, pH 8.0, 150 mM NaCl, 1 mM DTT).

To purify SiaC-His and SiaC^{T68A}-His, the pET28a-*siaC* and pET28a-*siaC*^{T68A} were constructed and proteins were purified with 5-ml HisTrap HP column (GE Healthcare) using His buffer A and His buffer B according to manufacture's instructions. To purify phosphorylated SiaC-His (SiaC^P-His), 10 mg purified SiaC-His protein was treated with 2 mg purified SiaB for 4 h at room temperature in the presence of 1 mM ATP. After incubation, SiaC^P-His was separated by a 10/300 Superdex 200 size exclusion column equilibrated with SEC buffer.

GST pull-down assay

To verify the interaction between SiaC and SiaD, 100 μg purified GST-SiaC was mixed with 20-μl prewashed glutathione magnetic beads (Promega, Madison, USA) on a rotator for 2 h at 4°C before washed three times by reaction buffer (50 mM Tris-HCl, pH 8.0, 150 mM NaCl, 0.1% Triton X-100). To avoid non-specific interaction, the beads were then blocked with 5% skim milk (*m/v*) 1 h at 4°C before washed three times by reaction buffer. SiaD-Flag expressed in PAO1 harboring pMMB67EH-*siaD*-Flag was cultured in LB medium with 0.5 mM IPTG and 30-ml stationary phase bacterial cultures were collected and lysed by sonication (Scientz Biotechnology, Ningbo, China) in reaction buffer. After addition of cell lysate to the pre-blocked beads, binding was allowed to proceed on a rotator for 4 h at 4°C. The beads were then washed five times with reaction buffer. Retained proteins were detected by Western blotting

after SDS–PAGE. To determine SiaA–SiaC, SiaB–SiaC interactions, a similar strategy was applied.

To test the interaction between SiaB and SiaC or SiaC^{T68A}, 50 µg purified GST–SiaB was mixed with 15-µl prewashed glutathione magnetic beads on a rotator for 2 h at 4°C before washed three times by reaction buffer. To avoid non-specific interaction, the beads were then blocked with 5% skim milk (*m/v*) 1 h at 4°C before addition of purified SiaC–His, SiaC^P–His, or SiaC^{T68A}–His. After 6 times washing by reaction buffer, samples were subject to Western blotting assays. To test the interaction between SiaD and SiaC or SiaC^P, a similar strategy was applied using purified GST–SiaD, SiaC–His, and SiaC^P–His. For SiaB–SiaC^P interaction, experiments were performed in reaction buffer with or without 2 mM ADP. For SiaA–SiaC^P interaction, experiments were performed in reaction buffer with or without 10 mM MgCl₂.

To test the formation of SiaA–SiaC–SiaB, 50 µg purified GST–SiaA₃₈₆ was mixed with 15-µl prewashed glutathione magnetic beads on a rotator for 2 h at 4°C before washed three times by reaction buffer. To avoid non-specific interaction, the beads were then blocked with 5% skim milk (*m/v*) 1 h at 4°C before addition of purified SiaC–His. After 2-h incubation, cell lysates of DH5α containing SiaB–Flag were added and incubated for another 2 h. After six times washing by reaction buffer, samples were subjected to Western blotting assays. To test formation of SiaA–SiaC–SiaD (or SiaB–SiaC–SiaD), a similar strategy was applied using GST–SiaA₃₈₆ (or GST–SiaB), SiaC–His, and cell lysates of DH5α-containing SiaD–Flag.

Surface plasmon resonance (SPR) experiments

Surface plasmon resonance (SPR) experiments were performed to measure the binding kinetic parameters between proteins. After the activation of the surface using NHS and EDC (1:1, *v/v*), the protein was immobilized on a CM5 sensor chip (GE Healthcare) by using standard amine-coupling at 25°C with buffer PBS-P (20 mM phosphate buffer, 2.7 mM NaCl, 137 mM KCl, 0.05% surfactant P-20, pH 7.4). The protein concentration was fixed at 50 ng/µl, and the immobilization level of protein was about 5,000 RU (response unit, 1 RU response value is roughly equivalent to 1 pg/mm² change of the concentration of the bound substance on the chip surface). After coupling, unreacted NHS ester groups were blocked with ethanolamine. After equilibration by running buffer (10 mM Tris–HCl, 150 mM NaCl, 0.05% surfactant P-20, pH 7.5), different concentrations of analytes were serially injected into the channel to evaluate the binding kinetic parameters. A reference channel was only activated and blocked to eliminate compound unspecific binding to the surface of the chip. An extra wash with 2 mM NaCl was added to remove the last remaining sample in the pipeline. The on-rates and the off-rates of the compounds were obtained by fitting the data sets to 1:1 Langmuir binding model using the Biacore T200 Evaluation Software (GE Healthcare). For interaction of SiaA with SiaC or SiaC^P, SiaA₃₈₆ was immobilized and experiments were performed in buffer with 10 mM MgCl₂. For SiaB–SiaC^P interactions, SiaB was immobilized and experiments were performed in buffers with or without 2 mM ADP.

SiaD stabilization assays

Overnight culture of wild-type PAO1, *siaC* mutant harboring pUCP20-*siaD*-Flag plasmid was sub-cultured into fresh LB broth to

an OD₆₀₀ of 1.5, followed by treatment with 50 µg/ml streptomycin. Bacterial samples were collected at 0, 30, 60, 90, 120, 180 min, and subjected to SDS–PAGE and Western blotting.

Western blot analysis

Samples were subjected to electrophoresis on 12% or 15% SDS–PAGE and transferred onto polyvinylidene difluoride membranes. After blocking with 5% (*w/v*) skim milk in TBST buffer (50 mM Tris, 150 mM NaCl, 0.05% Tween-20, pH 7.4), membranes were incubated with the appropriate primary antibody: anti-Flag (Sigma, Germany), anti-GST (Zhongshan Golden Bridge Biotechnology, Beijing, China), anti-RNA pol α (Biolegend, California, USA). After three times wash in TBST buffer, the membranes were incubated with horseradish peroxidase-conjugated Rabbit (TransGen, Beijing, China, for GST) or Mouse (TransGen, for Flag and RNAP) antibodies. Signals were detected using the ECL kit following the manufacturer's specified protocol.

Quantification of c-di-GMP production

Synthesis of c-di-GMP was carried out in 50 mM Tris–HCl, pH 7.5, 150 mM NaCl, and 5 mM MgCl₂. Subsequently, 3.5 µM SiaD alone or 3.5 µM SiaD with 7 µM SiaC was added to the reaction mixture for 1 h at room temperature. Reactions using 0.35 µM WspR alone or 0.35 µM SiaD with 7 µM *siaC* for 10 min were used as a control. To test the effect of SiaB on the SiaD activation, 7 µM SiaC or SiaC^{T68A} was pre-incubated with 2 µM SiaB in the presence of ATP (1 mM) for 2 h at room temperature. Reactions were initiated by the addition of 50 µM GTP to the mixture and allowed to incubate 3 h at 37°C. Reactions were terminated by heating the samples at 95°C for 5 min. Precipitated proteins were removed by centrifugation after which the supernatant was filtered through a 0.22-mm membrane. 15 µl of sample was loaded for high-performance liquid chromatography (Shimadzu, Japan), with 254 nm as detection wavelength. Symmetry C18 Column (4.6 mm × 25 cm) (Waters) was used with solvent A (10 mM ammonium acetate in water) and solvent B (10 mM ammonium acetate in methanol) at a flow rate of 0.2 ml/min. Eluent gradient is as follows: 0–9 min with 1% B; 9–14 min with 15% B; 14–19 min with 25% B; 19–35 min with 1% B. For SiaD^{R130G}, a similar strategy was applied.

Quantification of intracellular c-di-GMP level

Extraction of c-di-GMP was conducted as previously described with some modifications (Chen *et al*, 2015). Bacterial culture was prepared in ABTGC growth medium in 37°C shaker, with three replicates for each strain. Bacterial cells were harvested at early stationary stage for c-di-GMP extraction. Briefly, cell pellets were washed by pre-chilled 1 mM ammonium acetate for twice and were soaked in extraction buffer (acetonitrile:methanol:H₂O 2:2:1) overnight. Thereafter, three cycles of snap freeze–thaw and ice water sonication were carried out to extract raw metabolites. High-speed centrifugation (1,080 g at 4°C for 20 min) was applied to separate metabolites from the raw extracts. The supernatant of each sample was concentrated by speed-vacuum centrifugation for LC-MS/MS analysis, and the pellets were used for protein quantification and sample normalization.

The c-di-GMP in samples and c-di-GMP standard were analyzed in negative full scan mode with liquid chromatography coupled to hybrid quadrupole-Orbitrap mass spectrometer (Thermo Scientific Q Exactive). Waters BEH C18 column (2.1 × 50 mm, 1.7 μm) was used to separate 5 μl samples with phase A (10 mM ammonium formate and 0.1% formic acid in H₂O) and phase B (0.1% formic acid in MeOH) as mobile phases, and the flow rate was 0.3 ml/min. The gradient was as follows: Phase B was increased to 60% in 4.5 min from 3% at initial, then held for 0.5 min, returned back to 3% and held for 1.2 min. The capillary temperature of HESI source was 320°C, and the spray voltages were both 3 KV in negative mode. The sheath gas and aux gas were 30 and 10 psi separately. The standard c-di-GMP at 1 μg/ml was injected after every six injections as quality control. Data were analyzed using Xcalibur 2.2 software (Thermo Scientific).

Determination of ATP hydrolysis activity

10 μM SiaB or its mutants, 30 μM SiaC or its mutants, and 30 μM ATP were added to reaction buffer (10 mM Tris-HCl, pH 8.0, 10 mM NaCl) at room temperature. After 40 min, the concentration of residual ATP was determined using ATP assay kit (Beyotime Biotechnology, Beijing, China; Su *et al.*, 2014). Briefly, the residual ATP concentration in the reaction buffer was determined by mixing the buffer with luciferase reagent. The emitted light was measured using a microplate luminometer. The amount of ATP hydrolyzed during reaction for each sample represents the activity for each sample. The relative activity of each sample was normalized to that of the sample using SiaB and SiaC. 1 mM EDTA was added to reaction buffer when indicated. To test whether Na⁺ is essential for the ATP hydrolysis of SiaB, purified SiaB and SiaC was desalted by ammonium phosphate buffer (50 mM ammonium phosphate, pH 7.5) before reaction initiation.

Mass spectrum

Upon SDS-PAGE fractionation, the band of interest was excised and subjected to in-gel trypsin digestion as previously described¹. Nano-flow reversed-phase LC separation was carried out on an EASY-nLC 1200 system (Thermo Scientific). The capillary column (75 μm × 150 mm) with a laser-pulled electrospray tip (Model P-2000, Sutter Instruments) was home-packed with 5 μm, 100 Å Magic C18AQ silica-based particles (Michrom BioResources Inc., Auburn, CA). The mobile phase was composed of Solvent A (97% H₂O, 3% ACN, and 0.1% FA) and Solvent B (20% H₂O, 80% ACN and 0.1% FA). The LC separation was carried out at room temperature with the following gradient: Solvent B was started at 7% for 3 min and then raised to 40% over 40 min; subsequently, Solvent B was rapidly increased to 90% in 2 min and maintained for 10 min before 100% Solvent A was used for column equilibration. Eluted peptides from the capillary column were electrosprayed directly into a linear ion trap mass spectrometer (LTQ Velos Pro, Thermo Scientific) for MS and MS/MS analyses in a data-dependent acquisition mode. One full MS scan (*m/z* 400-1200) was acquired, and then, MS/MS analyses were performed on the 10 most intense ions. The selected ions were fragmented by collision-induced dissociation (CID) in the ion trap with the following parameters: ≥ +2 precursor ion charge, 2 Da precursor ion isolation window, and 35%

normalized collision energy. Dynamic exclusion was set with repeat duration of 24 s and exclusion duration of 12 s. Peptides and proteins were assigned by Mascot (2.3.02).

In vitro radioactive phosphorylation assays

For autokinase activity assays, full-length SiaB was incubated with 10 μCi [γ -³²P] ATP (PerkinElmer) in 20 μl of reaction buffer (10-mM Tris-HCl, pH 7.4, 50-mM KCl, 5-mM MgCl₂, 10% glycerol) for 1–5 min at room temperature.

To detect the phosphotransferase activity of SiaB toward SiaC/SiaC^{T68A}, and the phosphatase activity of SiaA, SiaB was autophosphorylated as above, and then, 10 μM of purified SiaC/SiaC^{T68A} and SiaA was added into the reaction mixture, which was incubated at room temperature for the appropriate time. The reaction was stopped with 5 × SDS-PAGE loading buffer. The phosphorylated proteins were separated by 12% SDS-PAGE. After electrophoresis, SDS-PAGE gels were dried by gel dryer and exposed to a X-OMAT BT Film (Kodak) for 3 h. After autoradiography, gels were stained by Coomassie Brilliant Blue to check the protein amounts.

Crystallization and data collection

Both SiaC and Se-substituted SiaB/SiaC samples in gel filtration buffer were concentrated to 10 mg/ml. The crystallization samples of SiaB/SiaC were prepared by mixing SiaB/SiaC and 2 mM ATP. The crystallization conditions were identified at 18°C using the Gryphon crystallization robot system from Art Robbins Instrument company and crystallization kits from Hampton Research Company. The apo-SiaC crystals were grown in buffer composed of 0.4 M NaH₂PO₄/1.6 M K₂HPO₄, 0.1 M imidazole pH 8.0, 0.2 M NaCl. The crystals of SiaB/SiaC complex were grown in 0.1 M Bis-Tris pH 6.5, 25% PEG 3350. All crystals were cryoprotected using their mother liquor supplemented with 25% glycerol and snap-frozen in liquid nitrogen. X-ray diffraction data (Appendix Table S1) were collected on beamline BL17U and BL19U at the Shanghai Synchrotron Radiation Facility (SSRF). Data processing was carried out using the HKL2000 or XDS programs (Minor *et al.*, 2006).

Structure determination and refinement

The phase of Se-substituted SiaB/SiaC structure was determined by single-wavelength anomalous diffraction (SAD) method (Giacovazzo & Siliqi, 2004) using the anomalous signal of Se- atoms with AutoSol program (Terwilliger *et al.*, 2009) embedded in the Phenix suite (Adams *et al.*, 2002). The initial model was refined using Refmac5 program (Murshudov *et al.*, 2011) of CPP4i suite (Potterton *et al.*, 2003). The apo-SiaC structure was solved by molecular replacement method; the SiaC molecule of the complex was used as search model. The model was manually built using COOT (Emsley & Cowtan, 2004) and refined using either Refmac5 or phenix.refine programs (Afonine *et al.*, 2012). During refinement, 5% of randomly selected data was set aside for free R-factor cross-validation calculations. The 2F_o-F_c and F_o-F_c electron density maps were regularly calculated and used as guides for building the missing amino acids and solvent molecules with COOT. The structural refinement statistics are summarized in Appendix Table S1.

Data availability

The atomic coordinates and structure factors for the reported crystal structures of SiaB-SiaC-ADP complex and SiaC have been deposited in the Protein Data Bank (PDB) under accession numbers 6KKO (<http://www.rcsb.org/pdb/explore/explore.do?structureId=6KKO>) and 6KKP (<http://www.rcsb.org/pdb/explore/explore.do?structureId=6KKP>).

Expanded View for this article is available online.

Acknowledgements

We are grateful to BL17U and BL19U beamline staff at the Shanghai Synchrotron Radiation Facility for their expert assistance during X-ray diffraction data collection. This work was supported the National Natural Science Foundation of China (31622003, 31670080, and 31870060 to HL and 31700064 to GC), Natural Science Basic Research Program of Shaanxi (2019JQ-134), the Program for Changjiang Scholars and Innovative Research Team in University (IRT1174 and ITR_15R55). We thank other members of the Liang laboratory for providing reagents, general support and critical reading of the manuscript. We thank Jing Wang and Qian Wang of Beijing University for help in SPR experiments.

Author contributions

GC and HL designed research. GC, YZ, JP, ML, WH, and YX performed the experiments. GC, CY, XD, and TW analyzed data; GC, JG, and HL wrote the paper.

Conflict of interest

The authors declare that they have no conflict of interest.

References

- Adams PD, Grosse-Kunstleve RW, Hung LW, Ioerger TR, McCoy AJ, Moriarty NW, Read RJ, Sacchettini JC, Sauter NK, Terwilliger TC (2002) PHENIX: building new software for automated crystallographic structure determination. *Acta Crystallogr D Biol Crystallogr* 58: 1948–1954
- Afonine PV, Grosse-Kunstleve RW, Echols N, Headd JJ, Moriarty NW, Mustyakimov M, Terwilliger TC, Urzhumtsev A, Zwart PH, Adams PD (2012) Towards automated crystallographic structure refinement with phenix.refine. *Acta Crystallogr D Biol Crystallogr* 68: 352–367
- Aravind L, Ponting CP (1999) The cytoplasmic helical linker domain of receptor histidine kinase and methyl-accepting proteins is common to many prokaryotic signalling proteins. *FEMS Microbiol Lett* 176: 111–116
- Baena I, Perez-Mendoza D, Sauviac L, Francesch K, Martin M, Rivilla R, Bonilla I, Bruand C, Sanjuan J, Lloret J (2019) A partner-switching system controls activation of mixed-linkage beta-glucan synthesis by c-di-GMP in *Sinorhizobium meliloti*. *Environ Microbiol* 21: 3379–3391
- Baraquet C, Murakami K, Parsek MR, Harwood CS (2012) The FleQ protein from *Pseudomonas aeruginosa* functions as both a repressor and an activator to control gene expression from the pel operon promoter in response to c-di-GMP. *Nucleic Acids Res* 40: 7207–7218
- Becher A, Schweizer HP (2000) Integration-proficient *Pseudomonas aeruginosa* vectors for isolation of single-copy chromosomal lacZ and lux gene fusions. *Biotechniques* 29: 948–950, 952
- Brencic A, Lory S (2009) Determination of the regulon and identification of novel mRNA targets of *Pseudomonas aeruginosa* RsmA. *Mol Microbiol* 72: 612–632
- Campbell EA, Masuda S, Sun JL, Muzzin O, Olson CA, Wang S, Darst SA (2002) Crystal structure of the *Bacillus stearothermophilus* anti-sigma factor SpoIIAB with the sporulation sigma factor sigmaF. *Cell* 108: 795–807
- Chen Y, Yuan M, Mohanty A, Yam JK, Liu Y, Chua SL, Nielsen TE, Tolker-Nielsen T, Givskov M, Cao B et al (2015) Multiple diguanylate cyclase-coordinated regulation of pyoverdine synthesis in *Pseudomonas aeruginosa*. *Environ Microbiol Rep* 7: 498–507
- Chew SC, Yam JKH, Matsyik A, Seng ZJ, Klebensberger J, Givskov M, Doyle P, Rice SA, Yang L, Kjelleberg S (2018) Matrix polysaccharides and siad diguanylate cyclase alter community structure and competitiveness of *Pseudomonas aeruginosa* during dual-species biofilm development with *Staphylococcus aureus*. *MBio* 6: e00585-18
- Cohen D, Mechold U, Nevenzal H, Yarmiyhu Y, Randall TE, Bay DC, Rich JD, Parsek MR, Kaever V, Harrison JJ et al (2015) Oligoribonuclease is a central feature of cyclic diguanylate signaling in *Pseudomonas aeruginosa*. *Proc Natl Acad Sci USA* 112: 11359–11364
- Colley B, Dederer V, Carnell M, Kjelleberg S, Rice SA, Klebensberger J (2016) SiaA/D interconnects c-di-GMP and RsmA signaling to coordinate cellular aggregation of *Pseudomonas aeruginosa* in response to environmental conditions. *Front Microbiol* 7: 179
- Emsley P, Cowtan K (2004) Coot: model-building tools for molecular graphics. *Acta Crystallogr D Biol Crystallogr* 60: 2126–2132
- Giacovazzo C, Siliqi D (2004) Phasing via SAD/MAD data: the method of the joint probability distribution functions. *Acta Crystallogr D Biol Crystallogr* 60: 73–82
- Guvener ZT, Harwood CS (2007) Subcellular location characteristics of the *Pseudomonas aeruginosa* GGDEF protein, WspR, indicate that it produces cyclic-di-GMP in response to growth on surfaces. *Mol Microbiol* 66: 1459–1473
- Hickman JW, Tifrea DF, Harwood CS (2005) A chemosensory system that regulates biofilm formation through modulation of cyclic diguanylate levels. *Proc Natl Acad Sci USA* 102: 14422–14427
- Hoang TT, Karkhoff-Schweizer RR, Kutchma AJ, Schweizer HP (1998) A broad-host-range Flp-FRT recombination system for site-specific excision of chromosomally-located DNA sequences: application for isolation of unmarked *Pseudomonas aeruginosa* mutants. *Gene* 212: 77–86
- Hunter T (1995) Protein kinases and phosphatases: the yin and yang of protein phosphorylation and signaling. *Cell* 80: 225–236
- Irie Y, Borlee BR, O'Connor JR, Hill PJ, Harwood CS, Wozniak DJ, Parsek MR (2012) Self-produced exopolysaccharide is a signal that stimulates biofilm formation in *Pseudomonas aeruginosa*. *Proc Natl Acad Sci USA* 109: 20632–20636
- Jenal U, Reinders A, Lori C (2017) Cyclic di-GMP: second messenger extraordinaire. *Nat Rev Microbiol* 15: 271–284
- Kelley LA, Mezulis S, Yates CM, Wass MN, Sternberg MJ (2015) The Phyre2 web portal for protein modeling, prediction and analysis. *Nat Protoc* 10: 845–858
- Klebensberger J, Birkenmaier A, Geffers R, Kjelleberg S, Philipp B (2009) SiaA and SiaD are essential for inducing autoaggregation as a specific response to detergent stress in *Pseudomonas aeruginosa*. *Environ Microbiol* 11: 3073–3086
- Kulasakara H, Lee V, Brenic A, Liberati N, Urbach J, Miyata S, Lee DG, Neely AN, Hyodo M, Hayakawa Y et al (2006) Analysis of *Pseudomonas aeruginosa* diguanylate cyclases and phosphodiesterases reveals a role for bis-(3'-5')-cyclic-GMP in virulence. *Proc Natl Acad Sci USA* 103: 2839–2844
- Masuda S, Murakami KS, Wang S, Anders Olson C, Donigian J, Leon F, Darst SA, Campbell EA (2004) Crystal structures of the ADP and ATP bound

- forms of the *Bacillus* anti-sigma factor SpoIIAB in complex with the anti-sigma SpoIIAA. *J Mol Biol* 340: 941–956
- Meek RW, Cadby IT, Moynihan PJ, Lovering AL (2019) Structural basis for activation of a diguanylate cyclase required for bacterial predation in *Bdellovibrio*. *Nat Commun* 10: 4086
- Minor W, Cymborowski M, Otwinowski Z, Chruszcz M (2006) HKL-3000: the integration of data reduction and structure solution—from diffraction images to an initial model in minutes. *Acta Crystallogr D Biol Crystallogr* 62: 859–866
- Murshudov GN, Skubak P, Lebedev AA, Pannu NS, Steiner RA, Nicholls RA, Winn MD, Long F, Vagin AA (2011) REFMAC5 for the refinement of macromolecular crystal structures. *Acta Crystallogr D Biol Crystallogr* 67: 355–367
- Orr MW, Donaldson GP, Severin GB, Wang J, Sintim HO, Waters CM, Lee VT (2015) Oligoribonuclease is the primary degradative enzyme for pGpG in *Pseudomonas aeruginosa* that is required for cyclic-di-GMP turnover. *Proc Natl Acad Sci USA* 112: E5048–E5057
- Potterton E, Briggs P, Turkenburg M, Dodson E (2003) A graphical user interface to the CCP4 program suite. *Acta Crystallogr D Biol Crystallogr* 59: 1131–1137
- Quin MB, Berrisford JM, Newman JA, Basle A, Lewis RJ, Marles-Wright J (2012) The bacterial stressosome: a modular system that has been adapted to control secondary messenger signaling. *Structure* 20: 350–363
- Ravichandran A, Sugiyama N, Tomita M, Swarup S, Ishihama Y (2009) Ser/Thr/Tyr phosphoproteome analysis of pathogenic and non-pathogenic *Pseudomonas* species. *Proteomics* 9: 2764–2775
- Romling U, Galperin MY, Gomelsky M (2013) Cyclic di-GMP: the first 25 years of a universal bacterial second messenger. *Microbiol Mol Biol Rev* 77: 1–52
- Ross P, Weinhouse H, Aloni Y, Michaeli D, Weinberger-Ohana P, Mayer R, Braun S, de Vroom E, van der Marel GA, van Boom JH et al (1987) Regulation of cellulose synthesis in *Acetobacter xylinum* by cyclic diguanylic acid. *Nature* 325: 279–281
- Schmidt AJ, Ryjenkov DA, Gomelsky M (2005) The ubiquitous protein domain EAL is a cyclic diguanylate-specific phosphodiesterase: enzymatically active and inactive EAL domains. *J Bacteriol* 187: 4774–4781
- Schmidt A, Hammerbacher AS, Bastian M, Nieken KJ, Klockgether J, Merighi M, Lapouge K, Poschgan C, Kolle J, Acharya KR et al (2016) Oxygen-dependent regulation of c-di-GMP synthesis by SadC controls alginate production in *Pseudomonas aeruginosa*. *Environ Microbiol* 18: 3390–3402
- Simm R, Morr M, Kader A, Nimtz M, Romling U (2004) GGDEF and EAL domains inversely regulate cyclic di-GMP levels and transition from sessility to motility. *Mol Microbiol* 53: 1123–1134
- Su B, Ji YS, Sun XL, Liu XH, Chen ZY (2014) Brain-derived neurotrophic factor (BDNF)-induced mitochondrial motility arrest and presynaptic docking contribute to BDNF-enhanced synaptic transmission. *J Biol Chem* 289: 1213–1226
- Taylor SS, Kornev AP (2011) Protein kinases: evolution of dynamic regulatory proteins. *Trends Biochem Sci* 36: 65–77
- Terwilliger TC, Adams PD, Read RJ, McCoy AJ, Moriarty NW, Grosse-Kunstleve RW, Afonine PV, Zwart PH, Hung LW (2009) Decision-making in structure solution using Bayesian estimates of map quality: the PHENIX AutoSol wizard. *Acta Crystallogr D Biol Crystallogr* 65: 582–601
- Valentini M, Laventie BJ, Moscoso J, Jenal U, Filloux A (2016) The diguanylate cyclase HsbD intersects with the HptB regulatory cascade to control *Pseudomonas aeruginosa* biofilm and motility. *PLoS Genet* 12: e1006354
- Vijay K, Brody MS, Fredlund E, Price CW (2000) A PP2C phosphatase containing a PAS domain is required to convey signals of energy stress to the sigmaB transcription factor of *Bacillus subtilis*. *Mol Microbiol* 35: 180–188
- West SE, Schweizer HP, Dall C, Sample AK, Runyen-Janecky LJ (1994) Construction of improved *Escherichia-Pseudomonas* shuttle vectors derived from pUC18/19 and sequence of the region required for their replication in *Pseudomonas aeruginosa*. *Gene* 148: 81–86
- Zhao J, Yu X, Zhu M, Kang H, Ma J, Wu M, Gan J, Deng X, Liang H (2016) Structural and molecular mechanism of CdpR involved in quorum-sensing and bacterial virulence in *Pseudomonas aeruginosa*. *PLoS Biol* 14: e1002449
- Zhu B, Liu C, Liu S, Cong H, Chen Y, Gu L, Ma LZ (2016a) Membrane association of SadC enhances its diguanylate cyclase activity to control exopolysaccharides synthesis and biofilm formation in *Pseudomonas aeruginosa*. *Environ Microbiol* 18: 3440–3452
- Zhu M, Zhao J, Kang H, Kong W, Liang H (2016b) Modulation of type III secretion system in *Pseudomonas aeruginosa*: involvement of the PA4857 gene product. *Front Microbiol* 7: 7